AD-A111 455 NAVAL RESEARCH LAB WASHINGTON DC F/G 20/5
COLLECTIVE EFFECTS ON THE OPERATION OF FREE ELECTRON LASERS WIT--ETC(U)
FEB 82 H P FREUND, P SPRANGLE, D DILLENBURG
UNCLASSIFIED NRL-MR-4763 NL

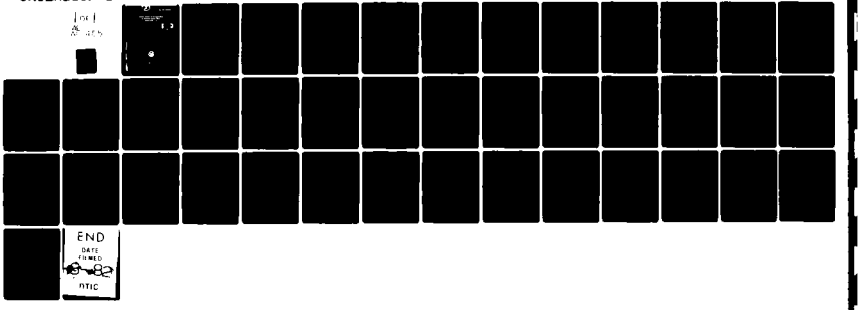

END
DATE FILMED
DTIC

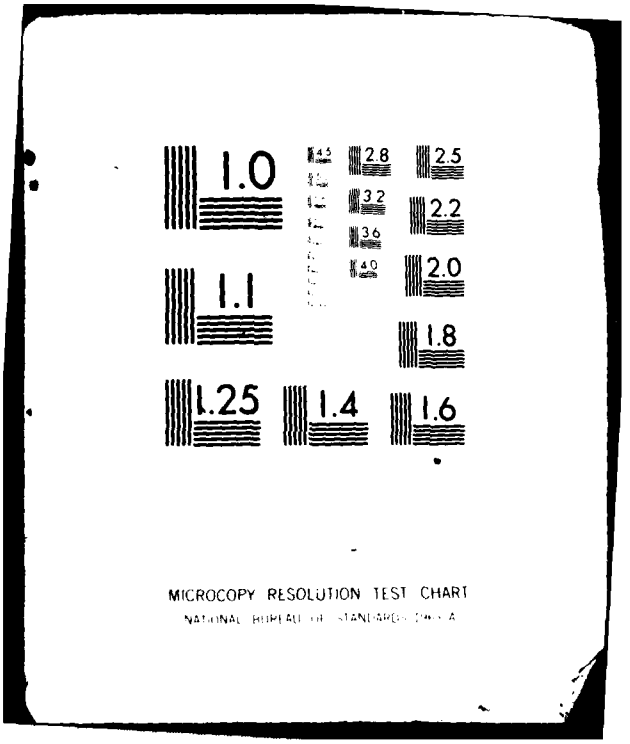
1.0
1.1
1.25
1.4
1.6
1.8
2.0
2.2
2.5
2.8
3.2
3.6
4.0
MICROCOPY RESOLUTION TEST CHART

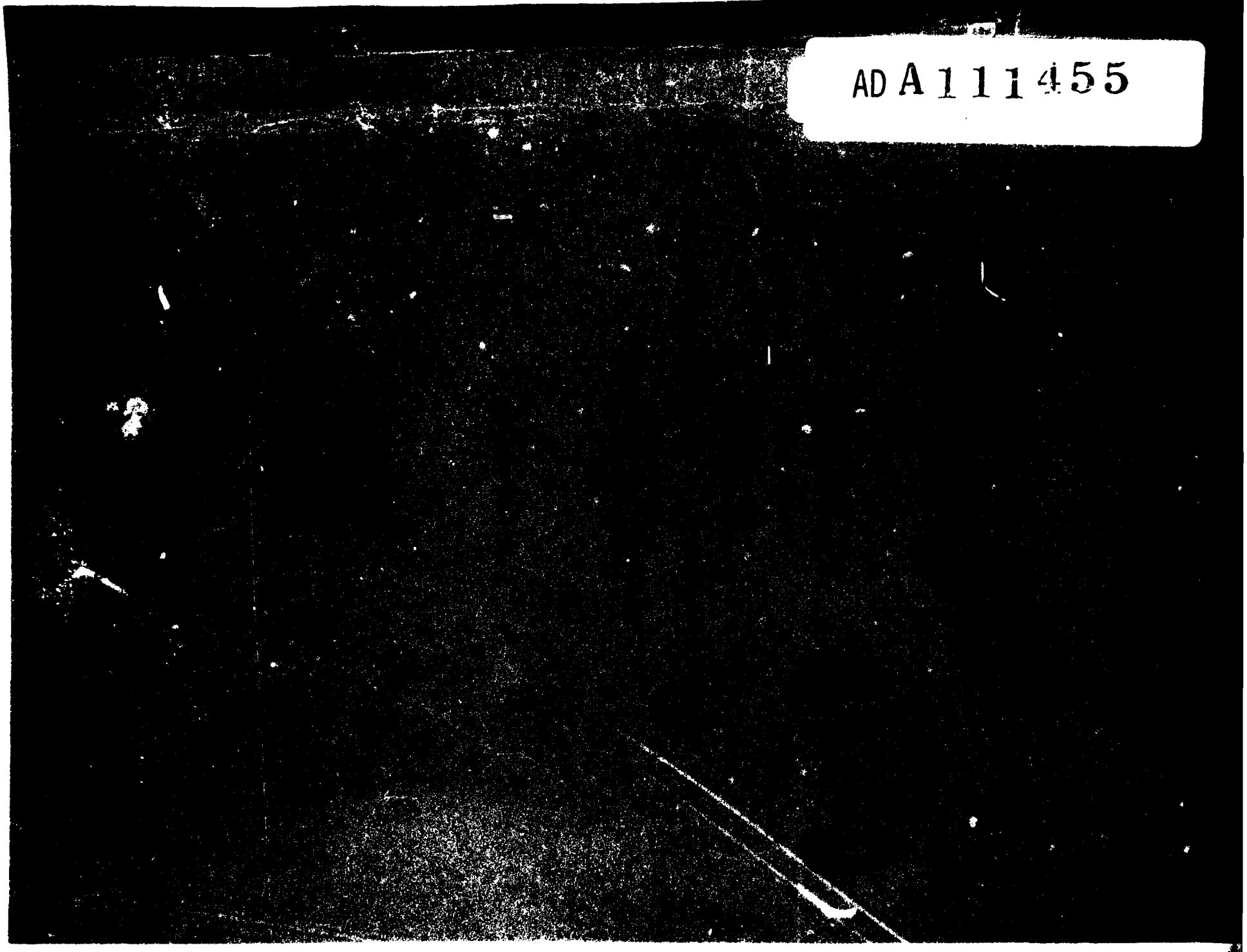

SECURITY CLASSIFICATION OF THIS PAGE (When Data Entered)

REPORT DOCUMENTATION PAGE	READ INSTRUCTIONS BEFORE COMPLETING FORM
1. REPORT NUMBER: NRL Memorandum Report 4763	2. GOVT ACCESSION NO.: AD-A111 455
3. RECIPIENT'S CATALOG NUMBER	
4. TITLE (and Subtitle): COLLECTIVE EFFECTS ON THE OPERATION OF FREE ELECTRON LASERS WITH AN AXIAL GUIDE FIELD	5. TYPE OF REPORT & PERIOD COVERED: Interim report on a continuing problem.
6. PERFORMING ORG. REPORT NUMBER	
7. AUTHOR(s): H. P. Freund,† P. Sprangle, D. Dillenburg,* E. H. da Jornada,* R. S. Schneider,* and B. Liberman*	8. CONTRACT OR GRANT NUMBER(s)
9. PERFORMING ORGANIZATION NAME AND ADDRESS: Naval Research Laboratory, Washington, D.C. 20375	10. PROGRAM ELEMENT, PROJECT, TASK AREA & WORK UNIT NUMBERS: 47-0920-0-1, WF32-389-592
11. CONTROLLING OFFICE NAME AND ADDRESS: U.S. Department of Energy, Washington, D.C. 20545	12. REPORT DATE: February 19, 1982
	13. NUMBER OF PAGES: 40
14. MONITORING AGENCY NAME & ADDRESS (if different from Controlling Office)	15. SECURITY CLASS. (of this report): UNCLASSIFIED
	15a. DECLASSIFICATION/DOWNGRADING SCHEDULE

16. DISTRIBUTION STATEMENT (of this Report)

Approved for public release; distribution unlimited.

17. DISTRIBUTION STATEMENT (of the abstract entered in Block 20, if different from Report)

18. SUPPLEMENTARY NOTES

†Science Applications, Inc., McLean, VA 22102

*Instituto de Fisica, Universidade Federal do Rio Grande do Sul, 90.000 Porto Alegre-RS, Brazil

19. KEY WORDS (Continue on reverse side if necessary and identify by block number)

Raman scattering
Free electron lasers
Coherent radiation
Millimeter waves

20. ABSTRACT (Continue on reverse side if necessary and identify by block number)

The collective interaction in a free electron laser with combined helical wiggler and uniform axial guide fields is presented in the linearized regime. The analysis involves a perturbation of the Vlasov-Maxwell equations about the constant-velocity helical trajectories, and the general driving currents are derived for this configuration. The complete dispersion equation is then obtained for a monoenergetic beam. Analytic solutions are obtained in the strong pump and space-charge dominated regimes, and an extensive numerical analysis is presented for a wide range of operating parameters. The results indicate that substantial enhancements in the gain are possible when the

(Continued)

DD FORM 1 JAN 73 1473 EDITION OF 1 NOV 65 IS OBSOLETE
S/N 0102-014-6601

SECURITY CLASSIFICATION OF THIS PAGE (When Data Entered)

20. ABSTRACT *(Continued)*

relativistic axial gyrofrequency is comparable to the Free Electron Laser Doppler Upshift. In addition, there is a range of parameters for which the ponderomotive potential acts to destabilize the electron beam. In this regime, we find both unstable electrostatic beam modes and largely electromagnetic modes with broad bandwidths.

CONTENTS

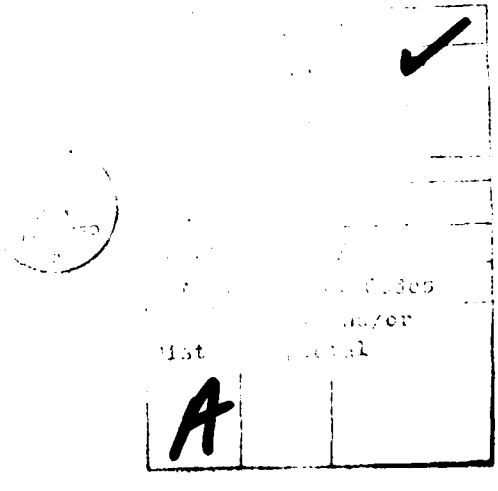

COLLECTIVE EFFECTS ON THE OPERATION OF FREE ELECTRON LASERS WITH AN AXIAL GUIDE FIELD

I. INTRODUCTION

The physical process which gives rise to wave amplification in free electron lasers stems from the interaction of a relativistic electron beam with a spatially periodic magnetic field (i.e., the wiggler or pump field) applied largely transverse to the direction of bulk electron motion. The effect of the wiggler field is to provide a coupling between the electron beam and electromagnetic radiation fields which results in a ponderomotive force along the axis of the beam. The form of the interaction can be classified in a variety of ways depending upon such parameters as the magnitude of the electron current, the strength of the pump field, the bulk energy and energy spread of the beam, and the length of the interaction region. For example, on the one hand thermal effects can be neglected when the energy spread in the beam $\Delta E << E_0/N$, where E_0 is the bulk beam energy and N is the number of wiggler periods in the interaction region. In this regime the entire electron beam participates in the interaction; however, collective (i.e., electrostatic) effects are important only when the fluctuating space-charge potential is comparable to the ponderomotive potential. The interaction in this collective regime is referred to as stimulated Raman scattering, and describes the coupling of a negative energy space-charge wave and a positive energy electromagnetic wave through the presence of the wiggler. On the other hand, when thermal effects are important, the radiation is resonant with only a small fraction of the beam and the process is termed stimulated Compton scattering. We shall be concerned in this paper with the cold beam limit, and deal with both the single-particle and collective regimes.

Manuscript submitted February 4, 1982.

An additional factor in the interaction is introduced by practical limitations in the propagation of intense electron beams; specifically, that an axial guide field is required to collimate intense beams in the transverse direction. This is of primary importance to free electron laser experiments operating at millimeter wavelengths[1-5] which employ relatively high current ($\gtrsim 1$ kA) and low energy (~ 1 MeV) electron beams. In contrast, an axial guide field is not a practical necessity for infrared free electron laser experiments[6-8] which typically operate at much lower ambient currents (~ 1 A) but higher energies (~ 50 MeV). However, the effect of the axial guide field on the free electron laser mechanism may be relevant in the latter case as well because of enhancements in the gain which may result when a guide field is present.

The effects of an axial guide field have been treated from the standpoints of both a fluid[9-13] and a kinetic[14-16] theory. It is our purpose in this work to treat the question of the free electron laser instability in the presence of an axial guide field in both the tenuous (i.e., single-particle regime) and dense (i.e., Raman regime) beam limits by means of a solution of the Vlasov-Maxwell equations. In the interest of analytic tractability a cold-beam approximation is imposed, and the contributions due to cyclotron mode interactions are included. The organization of the paper is as follows. In Sec. II, we develop the fluctuating source currents by solution of the Vlasov equation. The unperturbed orbits are assumed to be constant axial velocity (helical) trajectories,[17,18] and the source currents are found for a general equilibrium distribution. The general dispersion equation is obtained in Sec. III, and solved in several analytically accessible regimes for a cold beam limit. A detailed numerical solution is presented in Sec. IV for a wide range of operating parameters. A summary and discussion appears in Sec. V.

II. THE SOURCE CURRENT

In this section, we derive the fluctuating source current by means of solution of the linearized Vlasov equation. The physical configuration we consider is that of a relativistic electron beam propagating through an ambient magnetic field composed of a periodic helical wiggler field and a uniform axial guide field

$$\mathbf{B} = B_0\hat{\mathbf{e}}_z + \mathbf{B}_w(r, z), \tag{1}$$

where the wiggler field is assumed to be generated with a bifilar helix and is derived from a vector potential of the form[19]

$$\mathbf{A}_w = -\frac{2B_w}{k_w}\left[\frac{1}{k_w r} I_1(k_w r)\cos(\theta - k_w z)\hat{\mathbf{e}}_r - I_1'(k_w r)\sin(\theta - k_w z)\hat{\mathbf{e}}_\theta\right] \tag{2}$$

in cylindrical coordinates. In Eq. (2), B_w and k_w ($\equiv 2\pi/\lambda_w$, where λ_w is the wiggler period) are assumed to be constant and I_1 and I_1' are the modified Bessel function of the first kind and its derivative respectively. Since for most free electron laser experiments the initial beam radius is a small fraction of the wiggler period, we shall expand in powers of $k_w r$ and write

$$\mathbf{B}_w \simeq B_w(\hat{\mathbf{e}}_x \cos k_w z + \hat{\mathbf{e}}_y \sin k_w z). \tag{3}$$

The single-particle orbits in these combined fields have been amply discussed in the literature,[17,18] and will not be discussed in-depth here. We shall restrict consideration to orbits which are given approximately by stable helical trajectories, and write[15,18]

$$\begin{aligned} p_x &= \gamma m v_w \cos k_w z + P_x \cos \Omega_0 t - P_y \sin \Omega_0 t, \\ p_y &= \gamma m v_w \sin k_w z + P_x \sin \Omega_0 t + P_y \cos \Omega_0 t, \\ p_z &= \gamma m v_\parallel - \beta_w [P_x \cos(k_w z - \Omega_0 t) - P_y \sin(k_w z - \Omega_0 t)], \end{aligned} \tag{4}$$

where $v_w \equiv \Omega_w v_\parallel/(\Omega_0 - k_w v_\parallel)$ and $v_\parallel$ are the transverse and axial velocities corresponding to the helical trajectories, $\Omega_{0,w} \equiv |eB_{0,w}/\gamma mc|$, $\gamma \equiv (1 - v^2/c^2)^{-1/2}$, $\beta_w \equiv v_w/v_\parallel$ is the pump strength parameter, and P_x and P_y are constants which correspond to the canonical momenta in the limit as $B_0 \to 0$. Equations (4) are valid as long as $|\beta_w P_{x,y}| \ll |\gamma m v_\parallel|$ and require that v_w and $v_\parallel$ are related via

$$v_\parallel^2 + v_w^2 = (1 - \gamma^{-2})c^2, \tag{5}$$

which constitutes a quartic equation for $v_\parallel$. Equation (5) describes at most four distinct classes of trajectories of which one is characterized by motion antiparallel to $\mathbf{B}_0$ and will be ignored. Of the remaining trajectories having motion parallel to $\mathbf{B}_0$, we restrict consideration to those which are stable,[17,18] i.e., for which

$$(k_w v_\parallel - \Omega_0)[k_w v_\parallel - (1 + \beta_w^2)\Omega_0] > 0. \tag{6}$$

The typical dependence of the axial velocity on B_0 is shown in Fig. 1, in which we plot $\beta_{\parallel}(\equiv v_{\parallel}/c)$ versus β_0 $(\equiv \Omega_0/k_w c)$ for a kinetic energy of 1.5 MeV and wiggler amplitude and period such that $\Omega_w/k_w c = .05$. There are two classes of stable orbits. One class (referred to as group I) of orbits is characterized by high axial velocities and has $k_w v_{\parallel} > (1 + \beta_w^2)\Omega_0$. For these trajectories the axial velocity decreases monotonically with increasing B_0 until $v_{\parallel} = (1 + \beta_w^2)\beta_0 c$ which is the orbital stability boundary. For the parameters shown, this occurs for $\beta_0 \simeq .765$. The second class of orbits (group II) is characterized by an axial velocity which increases monotonically from zero with increasing B_0, and high axial velocities are, typically, found only when $\beta_0 \gtrsim 1$. In contrast to group I trajectories, the stability criterion (6) is satisfied for these orbits because $k_w v_{\parallel} < \Omega_0$. It will be shown in Sec. III that the relative magnitude of $k_w v_{\parallel}$ and Ω_0 for group I and II orbits has important consequences on the excited spectrum. Finally, it is important to note that $k_w v_{\parallel} \neq \Omega_0$ for either class of orbits. Were the equality to hold it would imply an infinite v_w which would violate the conservation of energy represented by Eq. (5).

The source current is obtained from the velocity moments of the perturbed distribution function $\delta f_b(z, \mathbf{p}, t) = f_b(z, \mathbf{p}, t) - F_b(P_x, P_y, p)$, where f_b is the complete distribution, F_b is the equilibrium distribution, and δf_b is assumed to be first order in the radiation fields. The formal solution of the Vlasov equation to this order is

$$\delta f_b(z, \mathbf{p}, t(z)) = e \int_0^z \frac{dz'}{v_z(z')} \left[\delta \mathbf{E}(z', t(z)) + \frac{1}{c}\, \mathbf{v}(z') \times \delta \mathbf{B}(z', t(z'))\right] \cdot \frac{\partial F_b}{\partial \mathbf{p}(z')}, \tag{7}$$

where the solution is parametrized in terms of the axial position relative to the start of the interaction region (at $z = 0$) and $t(z) = t_0 + \int_0^z dz'/v_z(z')$ is the sum of the time required for an electron to transverse the distance z and the entry time t_0.

We assume plane wave solutions of the form $\exp(-i\omega t)$ and choose to work with the scalar and vector potentials

$$\delta\phi(z, t) = \frac{1}{2}\, \delta\hat{\phi}(z) \exp(-i\omega t) + c.c.,$$

and

$$\delta \mathbf{A}(z, t) = \frac{1}{2}\delta \hat{\mathbf{A}}(z) \exp(-i\omega t) + c.c.,$$

where $\hat{\mathbf{e}}_z \cdot \delta \hat{\mathbf{A}}(z) = 0$. In addition, since the assumption of small P_x and P_y are implicit in the analysis, we adopt an equilibrium distribution of the form

$$F_b(P_x, P_y, p) = n_b \delta(P_x)\delta(P_y) G_b(p), \tag{8}$$

where n_b is the number density of the beam, and $G_b(p)$ is an arbitrary function subject to the normalization condition $\int_0^\infty dppG_p(p)/p_z = 1$. Observe that the choice of a distribution of this form (8) confines the equilibrium trajectories to be those constant axial velocity (helical) orbits described by (5). The interested reader is referred to Freund et al.[15] for a detailed derivation of the perturbed distribution and source current. We confine ourselves here to the final result. With respect to the basis $\hat{\mathbf{e}}_\pm = \frac{1}{2}(\hat{\mathbf{e}}_x \pm i\hat{\mathbf{e}}_y)$, the source current can be written in the form

$$\delta \mathbf{J}(z, t) = [\delta \hat{J}_+(z)\hat{\mathbf{e}}_+ + \delta \hat{J}_-(z)\hat{\mathbf{e}}_- + \delta \hat{J}_z(z)\hat{\mathbf{e}}_z] \exp(-i\omega t) + c.c., \tag{9}$$

where

$$\delta \hat{J}_\pm(z) = \frac{\omega_b^2}{8\pi c}\int_0^\infty dp\, \frac{p}{\gamma p_z}\left\{\exp(\mp i\Omega_0 t(z))\left(2 + \frac{p_+p_-}{p_z^2}\right)D_\pm + \exp(\pm i\Omega_0 t(z))\,\frac{p_\pm^2}{p_z^2}\,D_\mp \right.$$
$$\left. + p_\pm\left(\frac{\partial}{\partial P_x} + i\frac{\partial}{\partial P_y}\right)D_+ + p_\pm\left(\frac{\partial}{\partial P_x} - i\frac{\partial}{\partial P_y}\right)D_- - p_\pm D_z\frac{\partial}{\partial p}\right\} G_b(p)\Big|_{P_x=P_y=0}. \tag{10}$$

and

$$\delta \hat{J}_z(z) = \frac{\omega_b^2}{8\pi c}\int_0^\infty dp\, \frac{p}{\gamma}\left\{\left(\frac{\partial}{\partial P_x} + i\frac{\partial}{\partial P_y}\right)D_+ + \left(\frac{\partial}{\partial P_x} - i\frac{\partial}{\partial P_y}\right)D_- - D_z\frac{\partial}{\partial p}\right\} G_b(p)\Big|_{P_x=P_y=0}. \tag{11}$$

In Eqs. (10) and (11), ω_b is the beam plasma frequency, $p_\pm \equiv p_x \mp ip_y$,

$$D_\pm \equiv -\exp[\pm i\Omega_0 t(z)]\{\delta \hat{A}_\pm(z) - \delta \hat{A}_\pm(0)\exp[i(\omega \mp \Omega_0)\tau(z, 0)]$$
$$\mp i\Omega_0 \int_0^z \frac{dz'}{v_z(z')}\delta \hat{A}_\pm(z')\exp[i(\omega \mp \Omega_0)\tau(z, z')]\}, \tag{12}$$

and

$$D_z \equiv \frac{\gamma mc}{p}\int_0^z dz' \exp[i\omega\tau(z, z')]\left\{-\partial_{z'}\delta\hat{\phi}(z') + \frac{i\omega}{c}\left(\frac{p_-}{p_z}\delta \hat{A}_+(z') + \frac{p_+}{p_z}\delta \hat{A}_-(z')\right)\right\}. \tag{13}$$

where $\tau(z, z') \equiv t(z) - t(z')$. Finally, we assume the spatial dependence of the fields to be

$$\delta \hat{A}_{\pm}(z) = \delta \hat{A}_{\pm}(0) \exp(ik_{\pm}z)$$

and

$$\delta\hat{\phi}(z) = \delta\hat{\phi}(0) \exp(ikz).$$

As a result, the source currents can be expressed as

$$\delta \hat{J}_{\pm}(z) = -\frac{\omega_b^2}{8\pi c}\delta \hat{A}_{\pm}(z)\left[2\left\langle\left\langle \frac{p}{p_z}\,\frac{\omega - k_{\pm}v_z}{\omega \mp \Omega_0 - k_{\pm}v_{\parallel}}\right\rangle\right\rangle + a_w^2 S_{\pm}(k_{\pm}, \omega)\right]$$
$$- a_w \frac{ck^2}{8\pi}\delta\hat{\phi}(z)e^{\mp ik_w z}\chi_a(k, \omega), \tag{14}$$

and

$$\delta \hat{J}_z(z) = -\frac{\omega k}{8\pi}\delta\hat{\phi}(z)\chi(k, \omega) - \frac{\omega k_w}{8\pi}a_w\left[\delta\hat{A}_{-}(z)\exp(ik_w z)\sigma_{+}(k_{+}, \omega)\right.$$
$$\left. + \delta\hat{A}_{-}(z)\exp(-ik_w z)\sigma_{-}(k_{-}, \omega)\right], \tag{15}$$

where $a_w \equiv eA_w/mc^2$, $\langle\langle(\cdots)\rangle\rangle \equiv \int_0^{\infty} dp\, G_b(p)(\cdots)$,

$$\chi(k, \omega) \equiv \frac{\omega_b^2}{k}\int_0^{\infty} dp\,\frac{m}{\omega - kv_{\parallel}}\,\frac{\partial G_b}{\partial p}, \tag{16}$$

$$\chi_a(k, \omega) \equiv \frac{\omega_b^2}{k}\int_0^{\infty} dp\,\frac{k_w v_{\parallel}}{k_w v_{\parallel} - \Omega_0}\,\frac{m}{\gamma(\omega - kv_{\parallel})}\,\frac{\partial G_b}{\partial p}. \tag{17}$$

$$S_{\pm}(k_{\pm}, \omega) \equiv \int_0^{\infty} dp\frac{p}{\gamma^3 p_{\parallel}}G_b(p)\,\frac{c^2k_w^2}{(k_w v_{\parallel} - \Omega_0)^2}\left[1\right.$$
$$\left. + \frac{\Omega_0}{k_w v_{\parallel} - \Omega_0}\left\{\frac{\omega \mp \Omega_0 \pm k_w v_{\parallel}}{\omega \mp \Omega_0 - kv_{\parallel}} - \frac{\omega \mp k_w v_{\parallel}}{\omega \mp k_w v_{\parallel} - k_{\pm}v_{\parallel}}\right\}\right]$$
$$- \omega c^2\int_0^{\infty} dp\,\frac{k_w^2 v_{\parallel}}{\gamma^2(k_w v_{\parallel} - \Omega_0)^2}\,\frac{m}{\omega \mp k_w v_{\parallel} - k_{\pm}v_{\parallel}}\,\frac{\partial G_p}{\partial p}. \tag{18}$$

$$\sigma_{\pm}(k_{\pm}, \omega) \equiv \frac{\omega_b^2}{\omega}\int_0^{\infty} dp\left[\frac{\omega}{\gamma(k_w v_{\parallel} - \Omega_0)}\,\frac{mv_{\parallel}}{\omega \mp k_w v_{\parallel} - k_{\pm}v_{\parallel}}\,\frac{\partial}{\partial p}\right.$$
$$\left. + \frac{p}{\gamma^2 p_{\parallel}}\,\frac{\Omega_0}{(k_w v_{\parallel} - \Omega_0)^2}\left\{\frac{\omega \mp k_w v_{\parallel}}{\omega \mp k_w v_{\parallel} - k_{\pm}v_{\parallel}} - \frac{\omega}{\omega \mp \Omega_0 - k_{\pm}v_{\parallel}}\right\}\right]G_b(p), \tag{19}$$

and it has been assumed that $G_b(p) = 0$ for $p = 0, \infty$. Observe that Eqs. (14)-(19) are equivalent to the result found by Sprangle and Smith[20] in the limit as $B_0 \to 0$.

III. THE DISPERSION EQUATION

The dispersion equation is obtained by substitution of the source currents [Eqs. (14)-(19)] into Maxwell's equations

$$\left(\partial_z^2 + \frac{\omega^2}{c^2}\right)\delta\hat{A}_\pm(z) = -\frac{4\pi}{c}\delta\hat{J}_\pm(z),$$
$$\partial_z\delta\hat{\phi}(z) = \frac{8\pi i}{\omega}\delta\hat{J}_z(z). \tag{20}$$

This results in a set of three coupled equations for the initial field amplitudes

$$\Lambda_\pm(k \mp k_w, \omega)\,\delta\hat{A}_\pm(0) + \frac{1}{2}a_w\frac{c^2k^2}{\omega^2}\chi_a(k, \omega)\,\delta\hat{\phi}(0) = 0,$$
$$[1 + \chi(k, \omega)]\,\delta\hat{\phi}(0) + a_w\frac{k_w}{k}[\delta\hat{A}_+(0)\sigma_+(k - k_w, \omega) \tag{21}$$
$$+ \delta\hat{A}_-(0)\sigma_-(k + k_w, \omega)] = 0,$$

where the wavelength matching conditions imply that $k_\pm = k \mp k_w$, and

$$\Lambda_\pm(k_\pm, \omega) \equiv 1 - \frac{c^2k_\pm^2}{\omega^2} - \frac{\omega_b^2}{\omega^2}\left\langle\frac{p}{\gamma p_z}\frac{\omega - k_\pm v_\parallel}{\omega \mp \Omega_0 - k_\pm v_\parallel}\right\rangle - \frac{\omega_b^2}{2\omega^2}a_w^2 S_\pm(k_\pm, \omega) \tag{22}$$

describes the dispersion properties of the pure electromagnetic modes in the combined wiggler and axial guide fields. The dispersion equation itself is found by setting the determinant of the matrix of coefficients of Eqs. (21) to zero, which yields

$$1 + \chi(k\,\omega) = \frac{a_w^2}{2}\frac{k_w}{k}\frac{c^2k^2}{\omega^2}\chi_a(k, \omega)\left[\frac{\sigma_+(k - k_w, \omega)}{\Lambda_+(k - k_w, \omega)} + \frac{\sigma_-(k + k_w, \omega)}{\Lambda_-(k + k_w, \omega)}\right]. \tag{23}$$

It is evident that Eq. (23) describes the coupling between the electrostatic beam mode with each of the electromagnetic modes.

In the interest of analytic tractability, we shall now assume that the electron beam is sufficiently cold that a monoenergetic distribution of the form

$$G_b(p) = \frac{p_z}{p}\delta(p - p_0) \tag{24}$$

can be employed. As mentioned previously, this is generally valid as long as the momentum spread $\Delta p \ll p_0/N$. Combination of (23) and (24) yields a dispersion equation of the form

$$(\omega - k v_{\parallel})^2 - \kappa^2 v_{\parallel}^2 = - \frac{\beta_w^2}{2} \frac{\omega_b^2}{\gamma} \left[\frac{\alpha_+(k - k_w, \omega)}{\epsilon_+(k - k_w, \omega)} + \frac{\alpha_-(k + k_w, \omega)}{\epsilon_-(k + k_w, \omega)} \right] \tag{25}$$

to second order in the wiggler amplitude, where all orbit quantities (i.e., $v_{\parallel}$, γ_z, β_w, etc.) are computed using p_0,

$$\kappa^2 v_{\parallel}^2 \equiv \frac{\omega_b^2}{\gamma \gamma_z^2} \Phi, \tag{26}$$

$$\epsilon_{\pm}(k_{\pm}, \omega) \equiv 1 - \frac{\omega_b^2 (\omega - k_{\pm} v_{\parallel})}{\gamma (\omega^2 - k_{\pm}^2 c^2) (\omega \mp \Omega_0 - k_{\pm} v_{\parallel})}, \tag{27}$$

and

$$\begin{aligned} \alpha_{\pm}(k \mp k_w, \omega) \equiv & \frac{1}{\omega^2 - (k \mp k_w)^2 c^2} \left\{ \beta_{\parallel}^2 (\omega^2 - k^2 c^2 - \omega_b^2/\gamma) \right. \\ & + \frac{\omega_b^2}{\gamma} \beta_{\parallel}^2 (\omega - k v_{\parallel})^{-2} [(1 - \Psi^2) (kc - \omega v_{\parallel}/c)^2 + \gamma_z^{-2} (1 - \Phi) (\omega^2 - k^2 c^2)] \\ & + \frac{\omega_b^2}{\gamma \omega} \frac{\Omega_0}{k_w v_{\parallel} - \Omega_0} \beta_{\parallel} (kc - \omega v_{\parallel}/c) \Psi \left[\frac{\omega \mp k_w v_{\parallel}}{\omega - k v_{\parallel}} - \frac{\omega}{\omega \mp \Omega_0 - (k \mp k_w) v_{\parallel}} \right] \\ & + \frac{\Omega_0}{k_w v_{\parallel} - \Omega_0} [(\omega - k v_{\parallel})^2 - \kappa^2 v_{\parallel}^2] \left[\frac{3\omega \mp k_w v_{\parallel}}{\omega - k v_{\parallel}} - \frac{\omega \mp \Omega_0 \pm k_w v_{\parallel}}{\omega \mp \Omega_0 - (k \mp k_w) v_{\parallel}} \right] \\ & \left. - \gamma_z^{-2} (1 - \Phi) [(\omega - k v_{\parallel})^2 - \kappa^2 v_{\parallel}^2] \frac{\omega}{\omega - k v_{\parallel}} \left[\frac{\omega - 2k v_{\parallel}}{\omega - k v_{\parallel}} + \frac{2\Omega_0}{k_w v_{\parallel} - \Omega_0} \right] \right\} \end{aligned} \tag{28}$$

In addition, we have defined

$$\Phi \equiv 1 - \frac{\Omega_0 \beta_w^2 \gamma_z^2}{(1 + \beta_w^2) \Omega_0 - k_w v_{\parallel}}, \tag{29}$$

and

$$\Psi \equiv 1 - \frac{\Omega_0}{\beta_{\parallel}(kc - \omega v_{\parallel}/c)} \frac{(1 + \beta_w^2) k_w v_{\parallel} - \omega}{(1 + \beta_w^2) \Omega_0 - k_w v_{\parallel}}. \tag{30}$$

In Eq. (25), $\epsilon_{\pm}(k \mp k_w, \omega)$ describes the circularly polarized electromagnetic modes in the absence of the wiggler, and the left-hand-side describes the electrostatic beam modes. Observe, however, that the presence of the wiggler modifies the natural electrostatic response frequency by a factor of Φ defined in (29).

The wiggler field, therefore, provides a coupling between the space-charge wave and either polarization state of the electromagnetic wave. We choose, without loss of generality, to focus on the coupling with the $\delta \hat{A}_-$ mode. As a consequence, we shall assume that $|\epsilon_+(k - k_w, \omega)| << |\epsilon_-(k +$

$k_w, \omega)|$ and neglect the term in $\epsilon_-^{-1}(k + k_w, \omega)$ in (25). If we assume in addition that $\omega_b^2/\gamma\omega^2 << 1$, then the dispersion equation can be cast into the substantially simpler form

$$[(\omega - k v_{\parallel})^2 - \kappa^2 v_{\parallel}^2]\left[\omega^2 - k_+^2 c^2 - \frac{\omega_b^2(\omega - k_+ v_{\parallel})}{\gamma(\omega - \Omega_0 - k_+ v_{\parallel})}\right]$$
$$= -\frac{\beta_w^2}{2}\frac{\omega_b^2}{\gamma}\left\{\beta_{\parallel}^2\left[\omega^2 - k^2c^2 - \frac{\omega_b^2(\omega - k_+ v_{\parallel})}{\gamma(\omega - \Omega_0 - k_+ v_{\parallel})}\right]\right.$$
$$\left. + \gamma_z^{-2}\omega^2(1 - \Phi) + \omega\Omega_0\frac{\omega - k v_{\parallel}}{\omega - \Omega_0 - k_+ v_{\parallel}}\right\}, \tag{31}$$

where we have written $k_+ = k - k_w$ for simplicity. Peak gain in (31) can be expected to occur near the intersections of the electrostatic and electromagnetic dispersion curves. A schematic representation of the dispersion relation is shown in Fig. 2 for $\Omega_0 > \omega_b/\gamma^{1/2}$. Evidently, high frequency interactions with the electrostatic beam mode can occur only in the positive ω and k_+ quadrant when $v_{\parallel} > 0$, and we shall restrict the analysis to this regime. It should be observed that the slope of the space-charge modes ($\omega = k_+ v_{\parallel} + k_w v_{\parallel} \pm \kappa v_{\parallel}$) is identical to the pure cyclotron mode ($\omega = k_+ v_{\parallel} + \Omega_0$), and the relative magnitudes of the $k_+ = 0$ intercepts of these curves determine which branch of the electromagnetic dispersion curve participates in the interaction. This point will be discussed in more depth at a later stage of the analysis.

The dispersion equation represented by (31) is a fifth degree polynomial in k. If we make the restriction that $k_+ > 0$, then (31) can be reduced to the following quartic equation

$$(k - \frac{\omega}{v_{\parallel}} - \kappa)(k - \frac{\omega}{v_{\parallel}} + \kappa)(k - k_w - K_+)(k - k_w - K_-) = -\frac{\beta_w^2}{4}\xi^2 k_w^2 \frac{\omega}{Kc}\beta_{\parallel}^{-1}$$
$$\times\left[\frac{\omega}{\gamma_z^2 v_{\parallel}}\Phi\left(k - k_w - \frac{\omega - \Omega_0}{v_{\parallel}}\right) - \frac{\Omega_0}{v_{\parallel}}\left(k - \frac{\omega}{v_{\parallel}}\right)\right], \tag{32}$$

where $\xi \equiv \omega_b/\gamma^{1/2}ck_w$ is the beam strength parameter, $c^2K^2 \equiv \omega^2 - \omega_b^2/\gamma$,

$$K_{\pm} \equiv \frac{1}{2}\left(K + \frac{\omega - \Omega_0}{v_{\parallel}}\right) \pm \frac{1}{2}\sqrt{\Delta K^2 + 2\xi^2 k_w^2 \frac{\Omega_0}{K v_{\parallel}}}, \tag{33}$$

and $\Delta K \equiv K - (\omega - \Omega_0)/v_{\parallel}$. It is clear that the nature of the interaction is strongly dependent upon

the sign of Φ, which affects the natural electrostatic response frequency of the plasma as well as mediating the ponderomotive force.[2] In the limit as $B_0 \to 0$, Φ approaches unity and (32) reduces to the well-known results in the limit of zero axial field.[20-22] The behavior of Φ when the guide field is finite, however, is strongly dependent on the type of orbit under consideration. The variation of Φ with β_0 is shown in Fig. 3 for the parameters used to generate the orbits in Fig. 1. As shown in the figure, $\Phi \geq 1$ for group I orbits and contains a singularity when $\Omega_0(1+\beta_w^2) = k_w v_{\parallel}$ which is the orbital stability boundary. In the case of group II orbits the magnitude of Φ is, typically, less than or of the order of unity, but Φ is negative for axial guide fields less than a critical magnitude given by $[1+\beta_w^2(1-\gamma_z^2)]\Omega_0 = k_w v_{\parallel}$. As B_0 increases beyond this critical value Φ approaches unity; however, it should be noted that β_w decreases monotonically with increasing B_0 in this regime. In either case in which $\Phi > 0$, the interaction is basically one in which a positive energy electromagnetic wave is coupled to a negative energy space-charge wave by the action of the wiggler. Neither wave is intrinsically unstable and growth occurs when the wiggler amplitude is above threshold. However, when Φ is less than zero κ is imaginary and the space-charge waves, themselves, comprise a complex conjugate pair $\omega = k v_{\parallel} \pm i|\kappa| v_{\parallel}$ one of which is unstable. As a result, we shall distinguish between these two possibilities and treat the solution to the dispersion equation when Φ is positive and negative separately.

A. $\Phi > 0$

In this regime we observe that the orbital stability criterion implies that

$$k_w v_{\parallel} > \Omega_0 \left[1 + \left(\frac{B_w}{B_0}\right)^{2/3}\right] \tag{34}$$

for group I orbits, and the requirement that Φ be positive leads to the condition that

$$k_w v_{\parallel} < \Omega_0 \left[1 - (\gamma_z^2 - 1)^{1/3}\left(\frac{B_w}{B_0}\right)^{2/3}\right] \tag{35}$$

for group II orbits. As a consequence, the intersection between the space-charge and electromagnetic modes occurs at frequencies greater (less) than $\Omega_0(1-\beta_{\parallel})^{-1}$ for group I (II) orbits when $\kappa v_{\parallel} \ll$

$|k_w v_{||} - \Omega_0|$. This condition is satisfied as long as $\Phi < \gamma_z \xi^{-1} (B_w/B_0)^{2/3}$ and, since $\xi << 1$ is implicitly assumed in order to neglect self-field effects, is a relatively weak constraint. A schematic representation of the interaction is shown in Figs. 4a and 4b for group I and II orbits in which we plot ω versus k_+ and the dotted line represents complex conjugate roots. It is the lower (i.e., $\omega = k v_{||} - \kappa v_{||}$) space-charge mode which produces the active coupling and wave growth since this is the negative energy mode. We note that from (34) and (35), the intersections are not close to the cyclotron line and occur approximately for $\omega \simeq ck_+ \simeq (k_+ + k_w) v_{||}$. This is the well-known free electron laser resonance at $k_+ \simeq 2\gamma_z^2 k_w \beta_{||}$.

If the beam strength parameter is sufficiently small that $\xi << \gamma_z (B_w/B_0)^{2/3}$ and $\gamma_z (B_w/B_0)^{2/3} \Phi^{1/2}$, then the cyclotron resonance effects can be neglected and the dispersion equation reduces to the cubic

$$\delta k (\delta k + 2\kappa)(\delta k - \Delta k) \simeq - \frac{\beta_w^2}{4} \xi^2 k_w^2 \beta_{||}^{-1} \Phi \frac{\omega}{\gamma_z^2 v_{||}} \tag{36}$$

where we have chosen $\delta k \equiv k - \omega/v_{||} - \kappa$, and $\Delta k \equiv k_w + K - \omega/v_{||} - \kappa$ is the frequency mismatch parameter. Equation (36) reduces to the result found by Sprangle and Smith[20] in the limit as $B_0 \rightarrow 0$, and corresponds to the limit discussed by Friedland and Fruchtman.[13]

The single-particle or "strong-pump" regime occurs when $|\delta k| >> |2\kappa|$. In this regime, (36) can be approximated by

$$\delta k^2 (\delta k - \Delta k) \simeq - \frac{\beta_w^2}{4} \xi^2 k_w \beta_{||}^{-1} \Phi \frac{\omega}{\gamma_z^2 v_{||}}. \tag{37}$$

Peak growth occurs when $\Delta k \simeq 0$, for which the complex roots are

$$(\delta k)_{max} \simeq \frac{1}{2} (\sqrt{3} \pm i) \left(\frac{\beta_w^2}{2} \xi^2 \beta_{||}^{-1} \Phi \right)^{1/3} k_w. \tag{38}$$

Therefore, self-consistency imposes the requirement that

$$\kappa << \frac{1}{16} \beta_w^2 \gamma_z^2 \beta_{||} k_w \tag{39}$$

in order for Eq. (37) to be valid. It is important to recognize that in this regime the coupling between

the electrostatic beam mode and the $\delta \hat{A}_+$ mode is relatively unimportant, and the strength of the pump and ponderomotive potential completely dominate the interaction. Because of this, (37) can be recovered in a much more direct manner by ignoring the space-charge potential in (21) and setting $\Lambda_-(k - k_w, \omega) = 0$.

In the opposite, or space-charge dominated (or stimulated Raman scattering), regime, $|\delta k| << |2\kappa|$ and space-charge effects are predominate. Here, the dispersion equation is of the form

$$\delta k^2 - \Delta k \delta k + \frac{\beta_w^2}{4} \gamma_z^2 \beta_\parallel \kappa\, k_w \simeq 0. \tag{40}$$

which has the solutions

$$\delta k \simeq \frac{1}{2}\Delta k \pm \frac{1}{2}\sqrt{\Delta k^2 - \beta_w^2 \gamma_z^2 \beta_\parallel \kappa\, k_w}. \tag{41}$$

Peak gain is found for $\Delta k \simeq 0$ in this regime as well and is

$$(\delta k)_{\max} \simeq \frac{1}{2} i \beta_w \gamma_z k_w \left| \beta_\parallel \frac{\kappa}{k_w} \right|^{1/2}. \tag{42}$$

The Raman regime, therefore, occurs when

$$\kappa >> \frac{1}{8} \beta_w^2 \gamma_z^2 \beta_\parallel k_w, \tag{43}$$

and requires relatively large beam currents.

B. $\Phi < 0$

As mentioned previously, the space-charge waves are intrinsically unstable in this regime and a relatively broadbanded spectrum of excited electrostatic/electromagnetic waves is expected to occur. In addition; since we are dealing with group II orbits

$$\Omega_0 \left| 1 - (\gamma_z^2 - 1)^{1/3} \left| \frac{B_w}{B_0} \right|^{2/3} \right| < k_w v_\parallel < \Omega_0, \tag{44}$$

and the possibility of a cyclotron mode interaction exists when $\gamma_z^2 - 1 << (B_0/B_w)^2$.

In the high frequency $\omega >> (1 - \beta_\parallel)^{-1} \Omega_0$ and high $k >> k_w$ regime, the space-charge waves are characterized by frequencies $\omega << ck_+$, and the cyclotron resonance contributions can be ignored when

$$\xi << \frac{\omega}{ck_w} |\Phi|^{1/2} \beta_{\parallel} \gamma_z^{-1} (\gamma_z^2 - 1)^{1/3} \left(\frac{B_w}{B_0} \right)^{2/3}. \tag{45}$$

In this regime we recover the cubic dispersion Eq. (36) found earlier (when $\Phi > 0$). For frequencies such that $|\Delta k| << \delta k$ the free-electron laser solutions are obtained [see, for example, Eqs. (37) and (40) for the strong-pump and space-charge dominated regimes]; however, for high frequency space-charge modes $|\Delta k| \simeq \omega(1 - \beta_{\parallel})/v_{\parallel} >> |\delta k|$. For these waves, the dispersion equation can be approximated by the quadratic

$$k^2 - 2\frac{\omega}{v_{\parallel}} k + \frac{\omega^2}{v_{\parallel}^2} + |\kappa|^2 \left[1 - \frac{\beta_w^2}{4} \beta_{\parallel} \gamma_z^2 (1 + \beta_{\parallel}) \right] \simeq 0, \tag{46}$$

which has been expressed in terms of k rather than δk for convenience. The solution

$$k \simeq \frac{\omega}{v_{\parallel}} \pm i|\kappa| \sqrt{1 - \frac{\beta_w^2}{4} \beta_{\parallel} \gamma_z^2 (1 + \beta_{\parallel})}, \tag{47}$$

is obviously a modified space-charge wave. It should be observed that the presence of the wiggler acts as a stabilizing influence, and for sufficiently strong pumps (i.e., $\beta_w^2 \beta_{\parallel} \gamma_z^2 (1 + \beta_{\parallel}) > 4$) the mode is stable.

In the opposite limit in which $\omega << (1 - \beta_{\parallel})^{-1} \Omega_0$, it is more difficult to satisfy condition (45), and the cyclotron resonance is of greater importance. This regime will be discussed in depth in Section IV in the context of a complete numerical solution of the dispersion equation.

IV. NUMERICAL ANALYSIS

In this section, we conduct an extensive numerical analysis of the quartic dispersion Eq. (32) for a beam characterized by $\gamma = 3.94$ (1.5 MeV) and $\xi = .1$, and a wiggler such that $\Omega_w / k_w c = .05$. Our procedure is to solve (32) for a wide range of axial field strengths in the vicinity of $\Omega_0 \simeq k_w c$ by self-consistently calculating $v_{\parallel}$ for each case and for both types of stable trajectory. As in Section III, we distinguish between the regimes for which Φ is positive and negative.

In the limits in which Φ is positive, the dispersion properties of (32) are qualitatively represented in Fig. 4 for orbits in groups I and II. The growth rates ($\mathrm{Im}\, k/k_w$) are plotted versus frequency for several appropriate values of β_0 in Figs. 5 and 6 for the two types of trajectory. Instability is found to occur for $\omega \simeq (1-\beta_{\parallel})^{-1} k_w v_{\parallel}$ which corresponds to the well-known free-electron laser resonance condition. The observation of decreasing (increasing) frequencies of instability with increasing axial field for group I (II) orbits can, therefore, be explained by examination of Fig. 1 in which it is seen that $v_{\parallel}$ decreases (increases) with increasing β_0.

The behavior of the peak growth rates for the two classes of orbits can also be readily explained. As shown in Fig. 7, the peak growth rate for group I orbits is a monotonically increasing function of B_0 up to the singularity at the orbital stability boundary (at $\beta_0 \simeq .765$ for this choice of parameters). This behavior is due to increases in both β_w and Φ with the axial field which results in increases in the effects of both the electrostatic/electromagnetic coupling and the ponderomotive potential. Observe, however, that the singularity is due solely to the character of Φ since β_w is everywhere finite. The scaling of the maximum growth rate with β_0 is also shown in Fig. 7 for group II trajectories. In this case, however, Φ is bounded by unity and increases monotonically from zero (at $\beta_0 \simeq 1.25$) with increasing axial fields. In addition, β_w decreases monotonically to zero with increasing B_0 for group II orbits since $\lim_{B_0 \to \infty} \beta_w = B_w/B_0$. As a consequence, the peak growth can be expected to initially increase from zero at $\beta_0 \simeq 1.25$, and to decrease again slowly to zero as the axial field becomes large. This behavior for the growth rates of each class of orbit is in qualitative agreement with that found previously in the context of a low gain theory.[15] Finally, since it is our intention to treat the collective regime, the parameters have been chosen to correspond to the space-charge dominated limit discussed in Section III and the numerical results for the peak gain can be recovered from Eq. (40) to within an error of a few percent.

Some care must be taken in the characterization of the dispersion properties of (32) when $\Phi < 0$. For low axial fields ($\beta_0 \lesssim .7$ for the parameters under consideration) both $v_{\parallel}$ and $|\Phi|$ are low and condition (43) is not well-satisfied when $\omega < (1-\beta_{\parallel})^{-1}\Omega_0$. This regime is illustrated in Figs. 8 and 9 in

which we plot ω/ck_w versus $\mathrm{Re}\, k_+/k_w$ and Imk/k_w versus ω/ck_w respectively for $\beta_0 = .5$. The dashed line in Fig. 8 corresponds to complex conjugate roots. Evidently, two instability regimes exist. At high frequencies, the modified space-charge wave discussed in Section III B is obtained with an asymptotic value (i.e., high-ω limit of $\mathrm{Im}\, k/k_w$) which agrees to within 1% of the predicted value in Eq. (45). The instability found at lower frequencies is difficult to treat analytically, and corresponds to a modified cyclotron mode.

For higher axial fields ($\beta_0 \gtrsim .7$), the character of the unstable modes is altered. As shown in Fig. 10, in which we plot ω/ck_w versus $\mathrm{Re}\, k_+/k_w$ for $\beta_0 = 1$, there are still two unstable regimes. While the higher frequency regimes corresponds to the modified space-charge mode in this case as well, the lower frequency instability requires some discussion. The growth rate in this regime is plotted as a function of frequency in Fig. 11 for $\beta_0 = .8$, 1, and 1.2. In each case, the peak in $\mathrm{Im}\, k/k_w$ observed for the lower frequency instability corresponds to the region shown in Fig. 10 in which the real part of the complex modes (dashed line) exceeds that of the waves which are purely real. Near the peak $\Delta k \simeq 0$, and the instability which results is a largely electromagnetic free electron laser interaction which (for our choice of parameters) agrees to within a few percent of the analytic expression for the peak growth rate (40) in the collective, or stimulated Raman scattering, limit. As the frequency decreases, $|\Delta k|$ increases and the character of the instability becomes increasingly electrostatic and we find an unstable modified space-charge wave for frequencies $\omega \gtrsim \Omega_0$.

V. SUMMARY AND DISCUSSION

In this paper we have analyzed the linear growth rate in both the single-particle and collective regimes of operation of a free electron laser configuration which contains a uniform axial guide field. The technique employed consists, essentially, of a Vlasov theory of the perturbations about constant-$v_\perp$ helical trajectories, and includes the effects of both stimulated Raman scattering with electrostatic beam modes and the effect of the ponderomotive potential due to the excited radiation. Analytic expressions for the growth rate in these two regimes are found and a comparison is made with a numerical solution

of the full dispersion equation. Substantial agreement is found between the analytical and numerical treatments. In addition, substantial qualitative agreement also exists between the present work, which is in the high gain regime, and the small signal theories.[11,15]

The results indicate that substantial enhancements in the growth rate of the free electron laser instability may be obtained by the inclusion of an axial guide field in which $\Omega_0 \simeq ck_w$, as a result of increases in both the transverse velocity and the ponderomotive potential. It should be pointed out, however, that the presence of the guide field also gives rise to instability in the electrostatic beam mode for group II orbits when $\Phi < 0$. Since this may have a degrading effect on beam quality and, in turn, on the operating efficiency, further study of this question is required.

A cyclotron mode interaction in the collective regime has been found only where the axial velocity and $|\Phi|$ are relatively small. However, two factors should be noted. The first is that our choice of equilibrium orbits (i.e., with $P_x = P_y = 0$) has intrinsically ignored the random (or Larmor) component of the transverse velocity which can be expected to be the primary source of a gyrotron type of instability. The second is our choice of an idealized magnetic field structure in which transverse gradients in the wiggler field have been neglected, which is valid only for orbits in which $k_w r << 1$. Since small $v_{\parallel}$ implies large transverse velocities and excursions from the axis of symmetry, the choice of an ideal wiggler ultimately breaks down in this limit.

ACKNOWLEDGMENTS

This work was supported, in part, under NAVAIR Contract No. WF32-389-592. In addition, support for several of us (D.D., E.H.J., B.L. and R.S.S.) was provided by the Conselho Nacional de Desenvolvimento Cientifico e Technologico and the Financiadora de Estudos e Projetos of Brazil.

REFERENCES

1. D.B. McDermott, T.C. Marshall, S.P. Schlesinger, R.K. Parker, and V.L. Granatstein, Phys. Rev. Lett. **41**, 1368 (1978).

2. S.H. Gold, R.H. Jackson, R.K. Parker, H.P. Freund, V.L. Granatstein, P.C. Efthimion, M. Herndon, and A.K. Kinkead, to appear in *Physics of Quantum Electronics*, Vol. 9 (eds. S.F. Jacobs, H.S. Pilloff, M. Sargent, M.O. Scully, and R. Spitzer, Addison-Wesley, New York, 1982).

3. R.E. Shefer and G. Bekefi, Bull. Am. Phys. Soc. **26**, 846 (1981).

4. C.W. Roberson, J. Pasour, F. Mako, R. Gilgenbach, and P. Sprangle, Bull. Am. Phys. Soc. **26**, 1016 (1981).

5. K. Felch, L. Vallier, and J.M. Buzzi, Bull. Am. Phys. Soc. **26**, 945 (1981).

6. L.R. Elias, W.M. Fairbank, J.M.J. Madey, H.A. Schwettman, and T.I. Smith, Phys. Rev. Lett. **36**, 717 (1976).

7. D.A.G. Deacon, L.R. Elias, J.M.J. Madey, G.J. Ramian, H.A. Schwettman, and T.I. Smith, Phys. Rev. Lett. **38**, 892 (1977).

8. H. Boehmer, M.Z. Caponi, J. Edighoffer, S. Fornaca, J. Munch, G. Neil, B. Saur, and C. Shih, Bull. Am. Phys. Soc. **26**, 853 (1981).

9. P. Sprangle, V.L. Granatstein, and L. Baker, Phys. Rev. A **12**, 1697 (1975).

10. T. Kwan and J.M. Dawson, Phys. Fluids **22**. 1089 (1979).

11. L. Friedland and J.L. Hirshfield, Phys. Rev. Lett. **44**, 1456 (1980).

12. I.B. Bernstein and L. Friedland, Phys. Rev. A. **23**, 816 (1981).

13. L. Friedland and A. Fruchtman, Bull. Am. Phys. Soc. **26**, 1016 (1981).

14. M.Z. Caponi, J. Munch, and M. Boehmer, in *Free Electron Generators of Coherent Radiation*, eds. S.F. Jacobs, H.S. Pilloff, M. Sargent, M.O. Scully, and R. Spitzer (Addison-Wesley, New York, 1980), p. 523.

15. H.P. Freund, P. Sprangle, D. Dillenburg, E.H. da Jornada, B. Liberman, and R.S. Schneider, Phys. Rev. A. **24**, 1965 (1981).

16. S. Johnston, to appear in *Physics of Quantum Electronics*, Vol. 9 (eds. S.F. Jacobs, H.S. Pilloff, M. Sargent, M.O. Scully, and R. Spitzer, Addison-Wesley, New York, 1982).

17. L. Friedland, Phys. Fluids **23**, 2376 (1980).

18. H.P. Freund and A.T. Drobot, Phys. Fluids (submitted for publication).

19. P. Diament, Phys. Rev. A. **23**, 2537 (1981).

20. P. Sprangle and R.A. Smith, Phys. Rev. A. **21**, 293 (1980).

21. I.B. Bernstein and J.L. Hirshfield, Phys. Rev. A. **20**, 1661 (1979).

22. R.C. Davidson and H.S. Uhm, Phys. Fluids **23**, 2076 (1980).

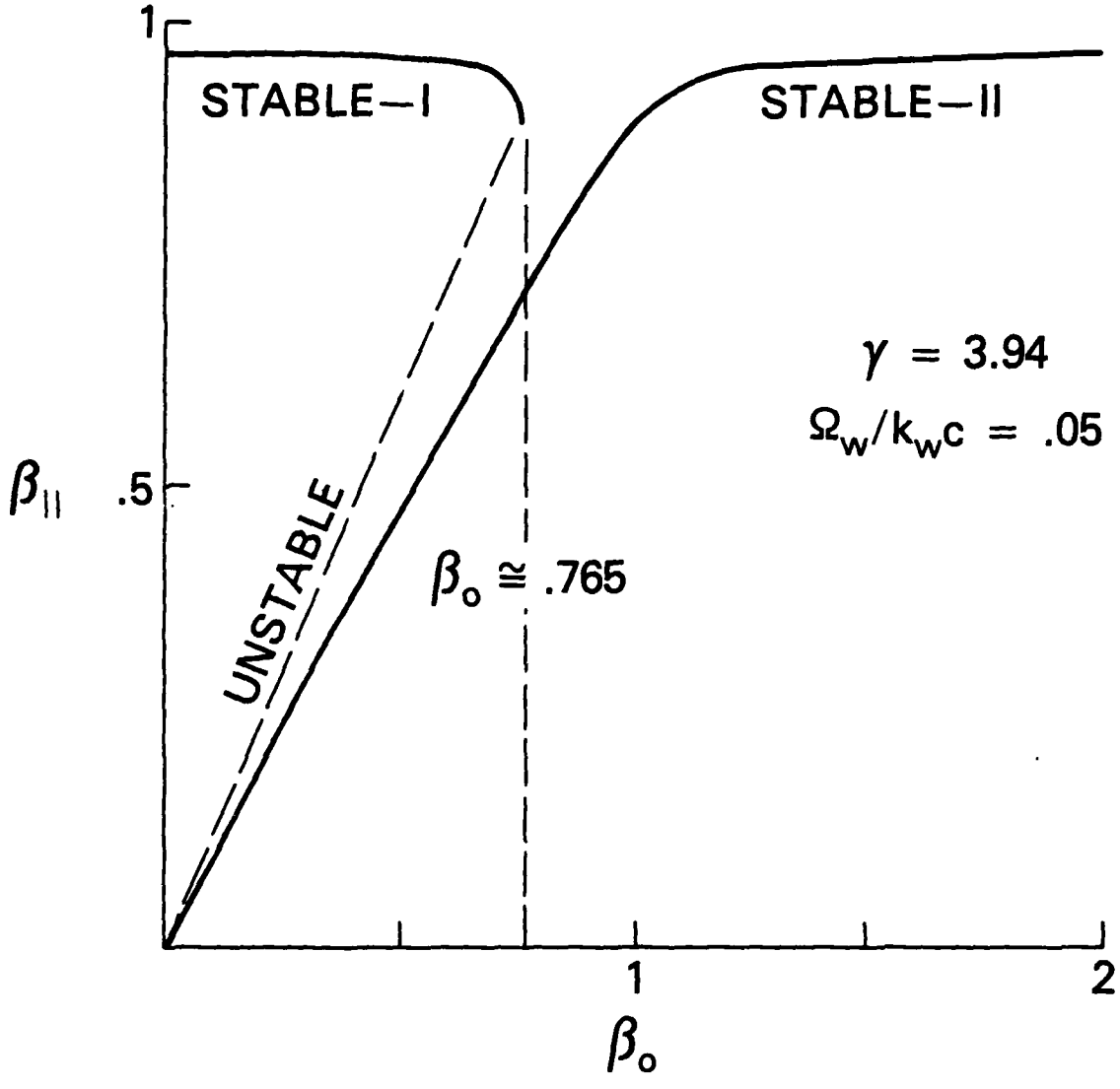

Fig. 1 — Graph of the axial velocity versus β_0 ($\equiv \Omega_0/k_w c$) for a beam energy of 1.5 MeV and a wiggler amplitude and period such that $\Omega_w/k_w c = .05$

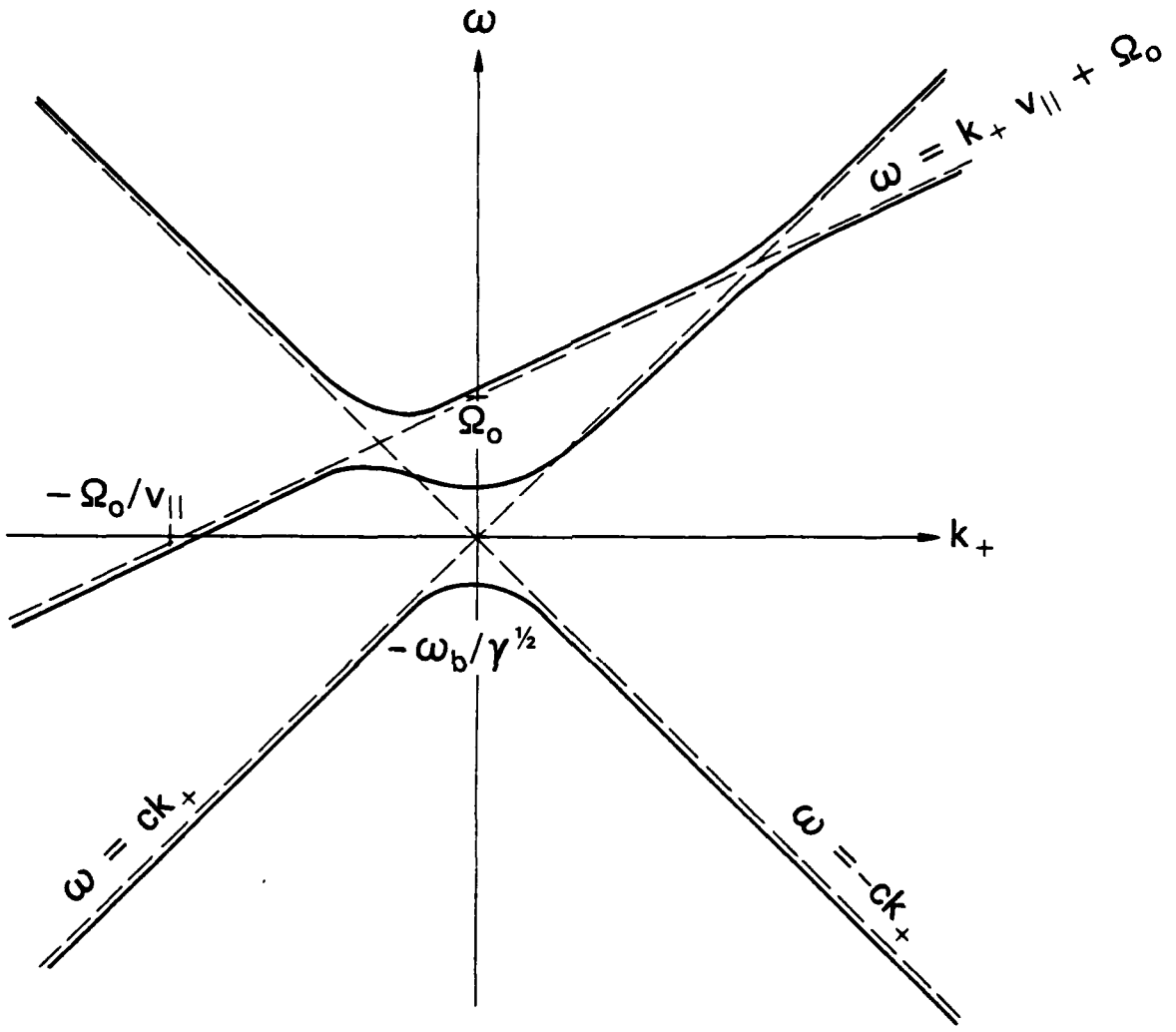

Fig. 2 — Schematic representation of the dispersion curves for the $\delta\hat{A}_\perp$ mode showing the passive interaction between the cyclotron and the pure electromagnetic mode at $\omega \simeq (1 - \beta_\parallel)^{-1}\Omega_0$

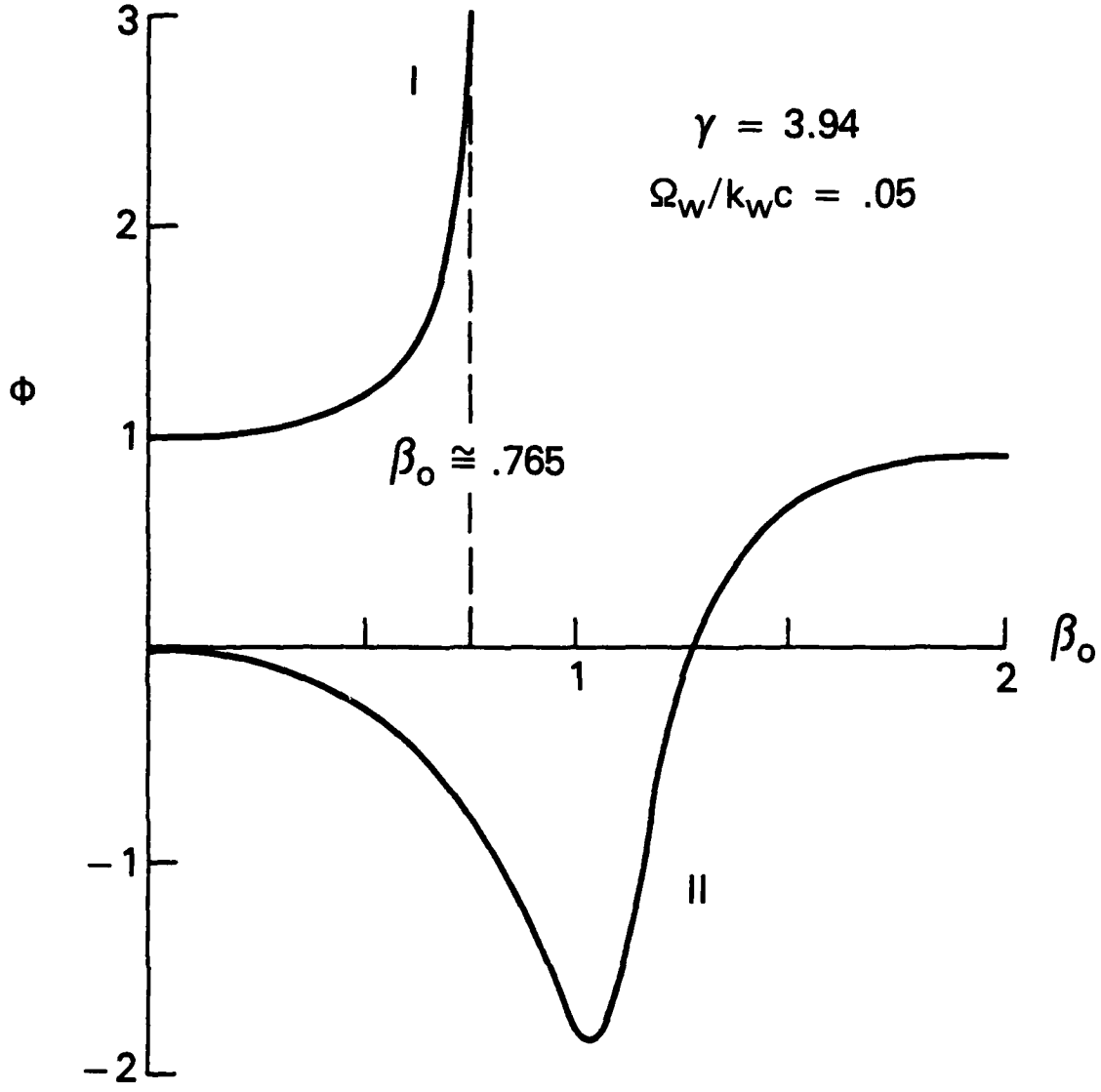

Fig. 3 — Graph of Φ versus β_0 for both group I and group II orbits for a beam energy of 1.5 MeV and a wiggler amplitude and period such that $\Omega_w/k_w c = .05$

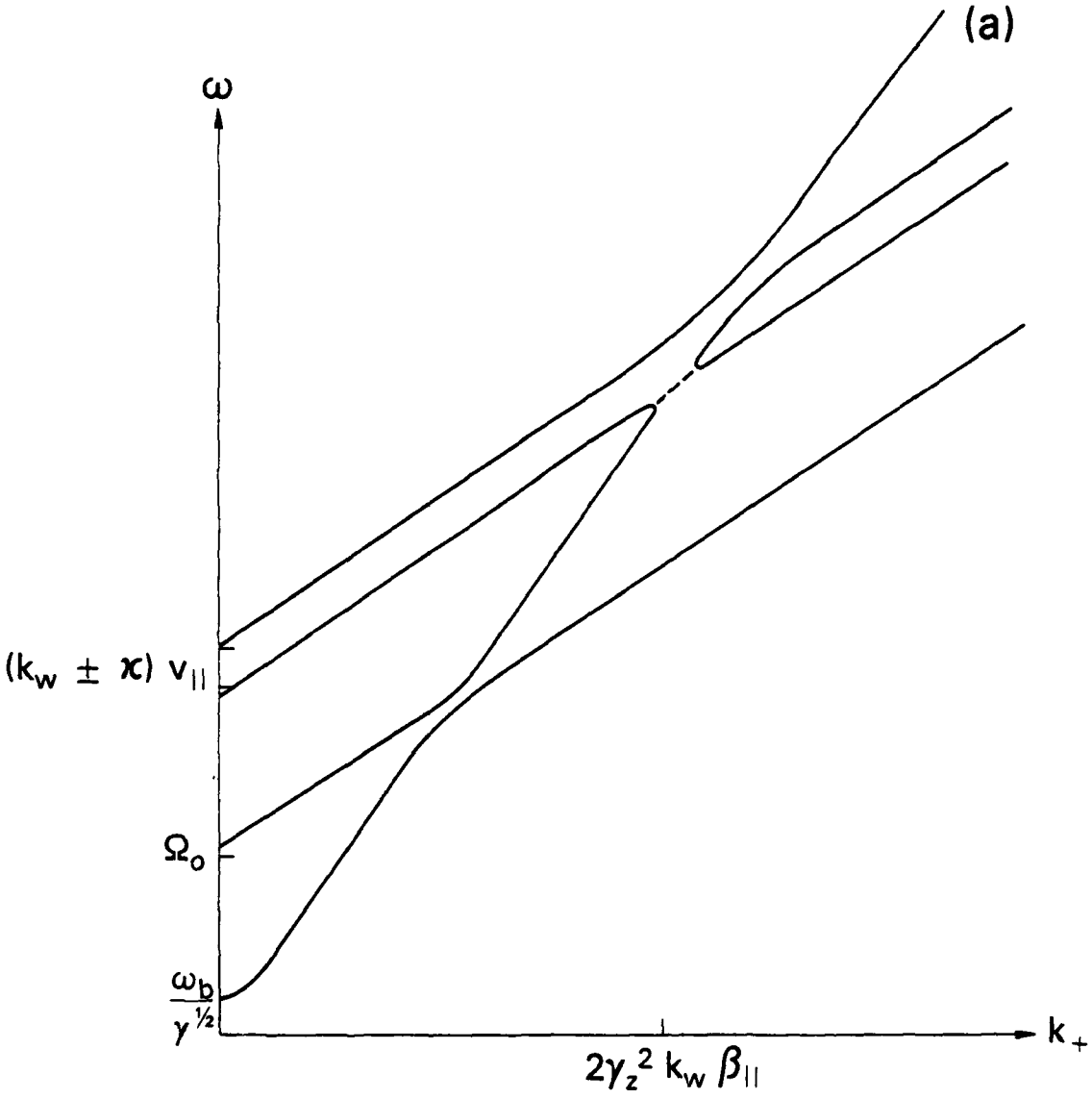

Fig. 4 — Schematic representation of the interaction for group I (a) and group II (b) orbits when $\Phi > 0$. The dotted line denotes complex conjugate roots.

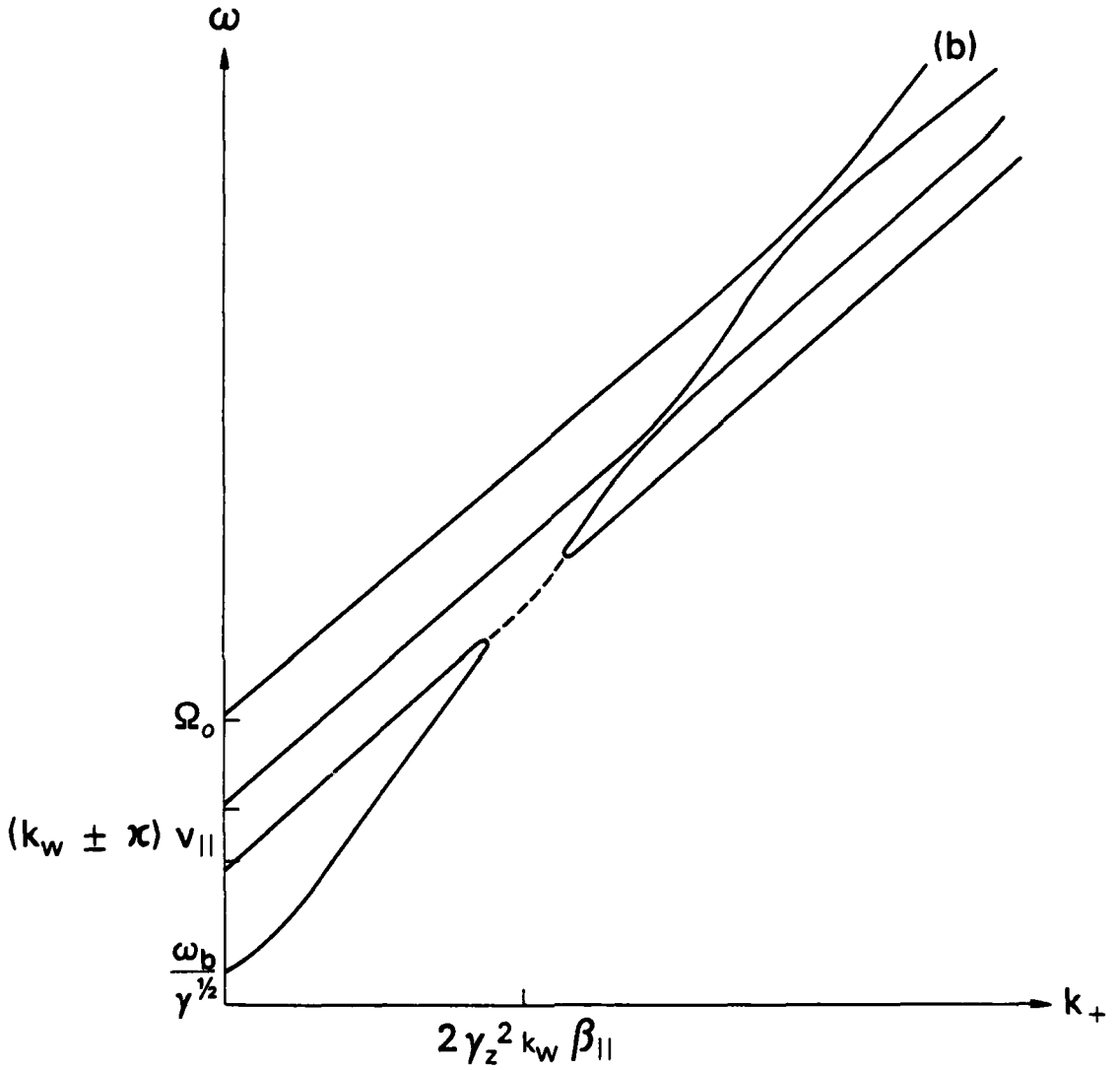

Fig. 4 (Continued) — Schematic representation of the interaction for group I (a) and group II (b) orbits when $\Phi > 0$. The dotted line denotes complex conjugate roots.

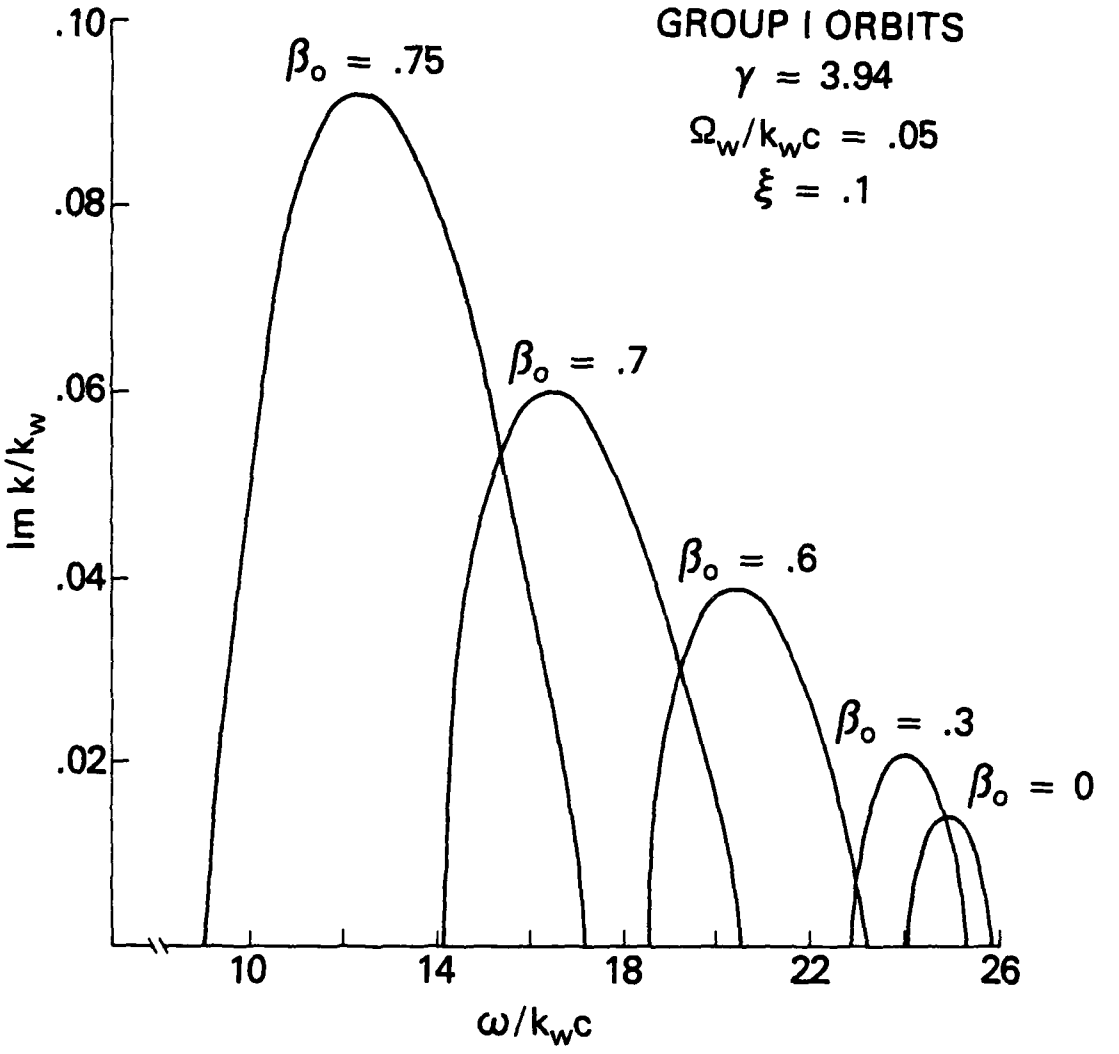

Fig. 5 — Graph of Im k/k_w versus $\omega/k_w c$ for group I orbits

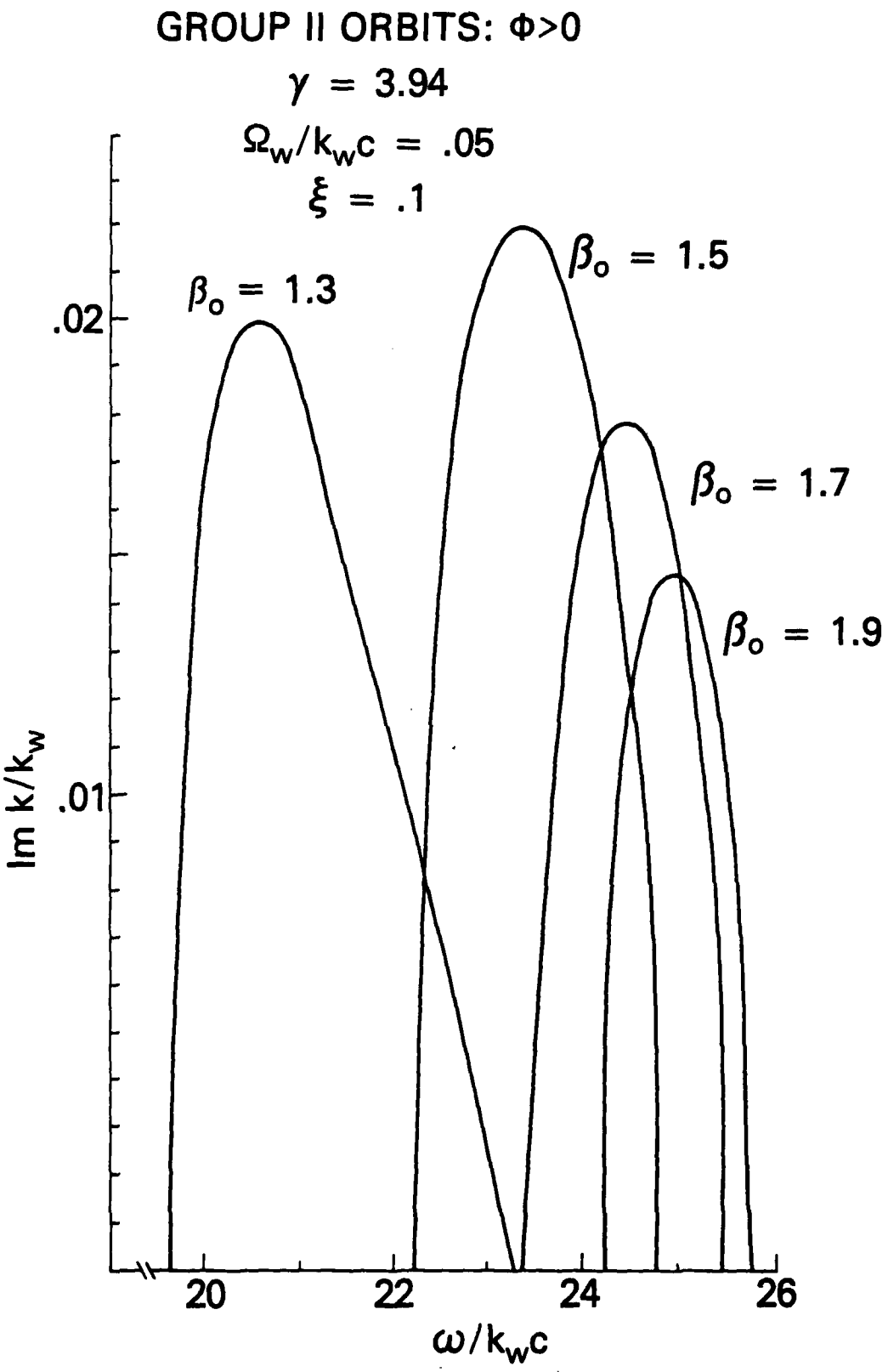

Fig. 6 — Graph of Im k/k_w versus $\omega/k_w c$ for group II orbits ($\Phi > 0$)

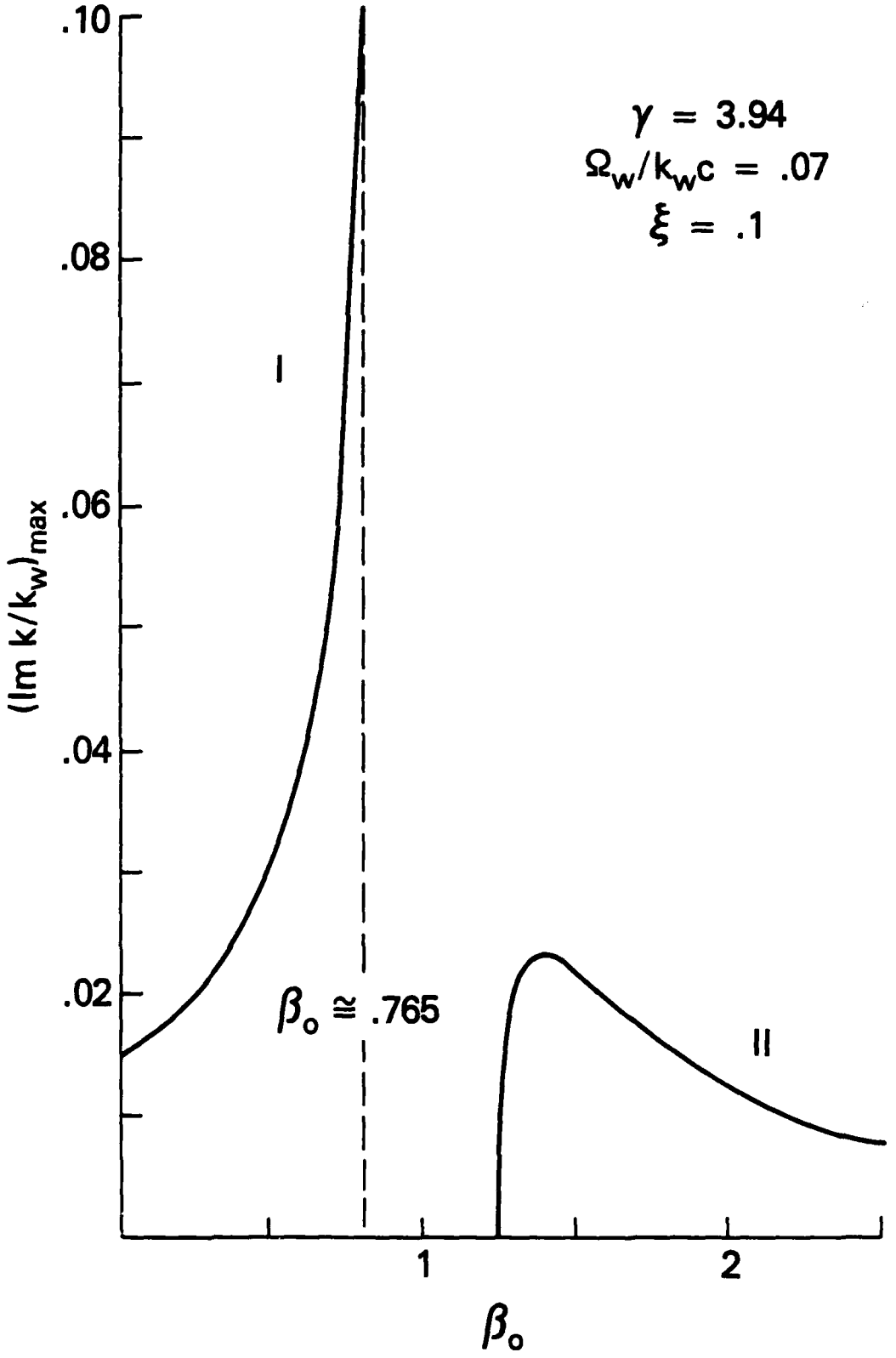

Fig. 7 — Graph of $(\mathrm{Im}\, k/k_w)_{max}$ as a function of the axial guide field for group I and II ($\Phi > 0$) orbits

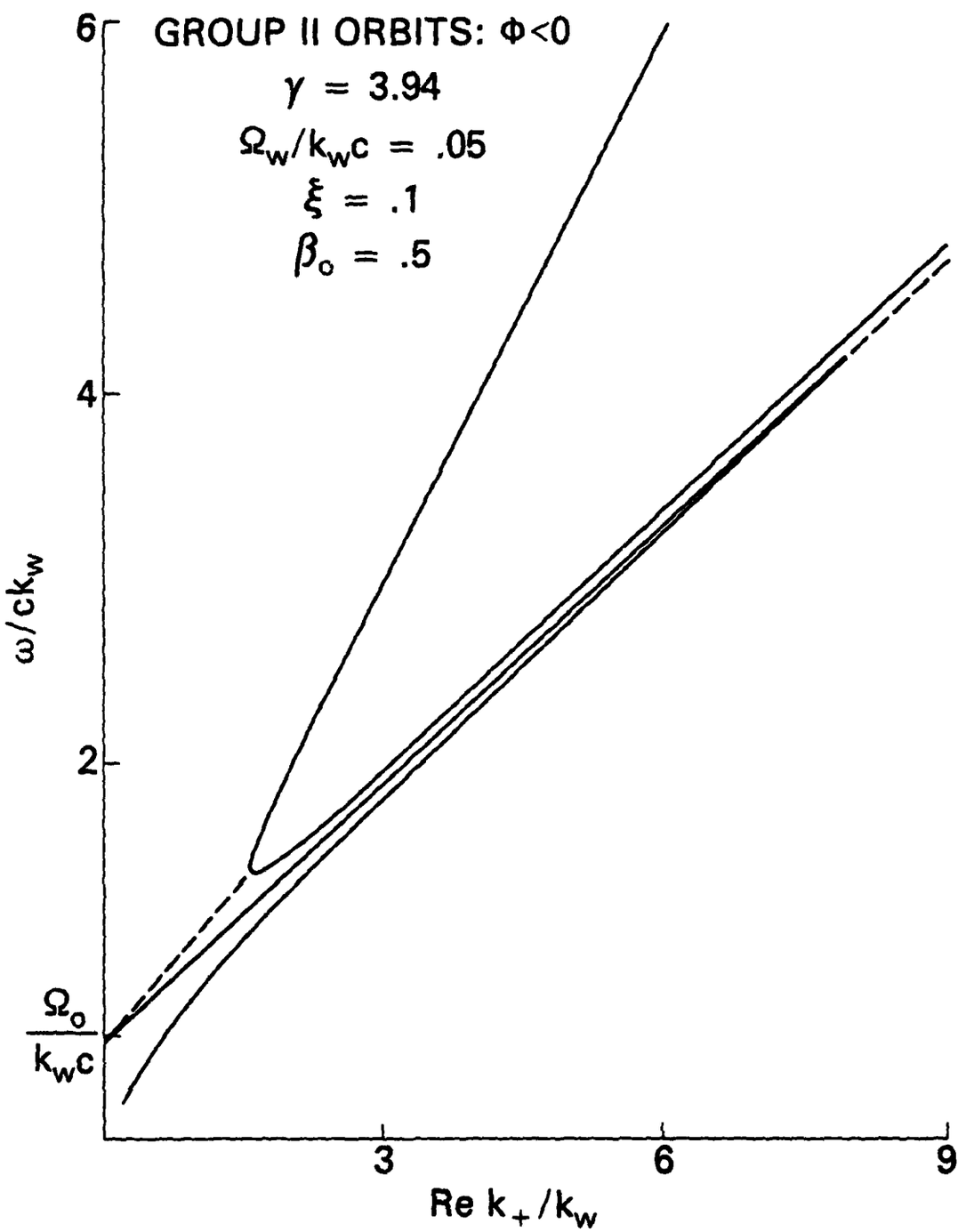

Fig. 8 — Graph of ω/ck_w versus $\mathrm{Re}\,k_+/k_w$ for group II orbits ($\Phi < 0$) and $\beta_0 = .5$

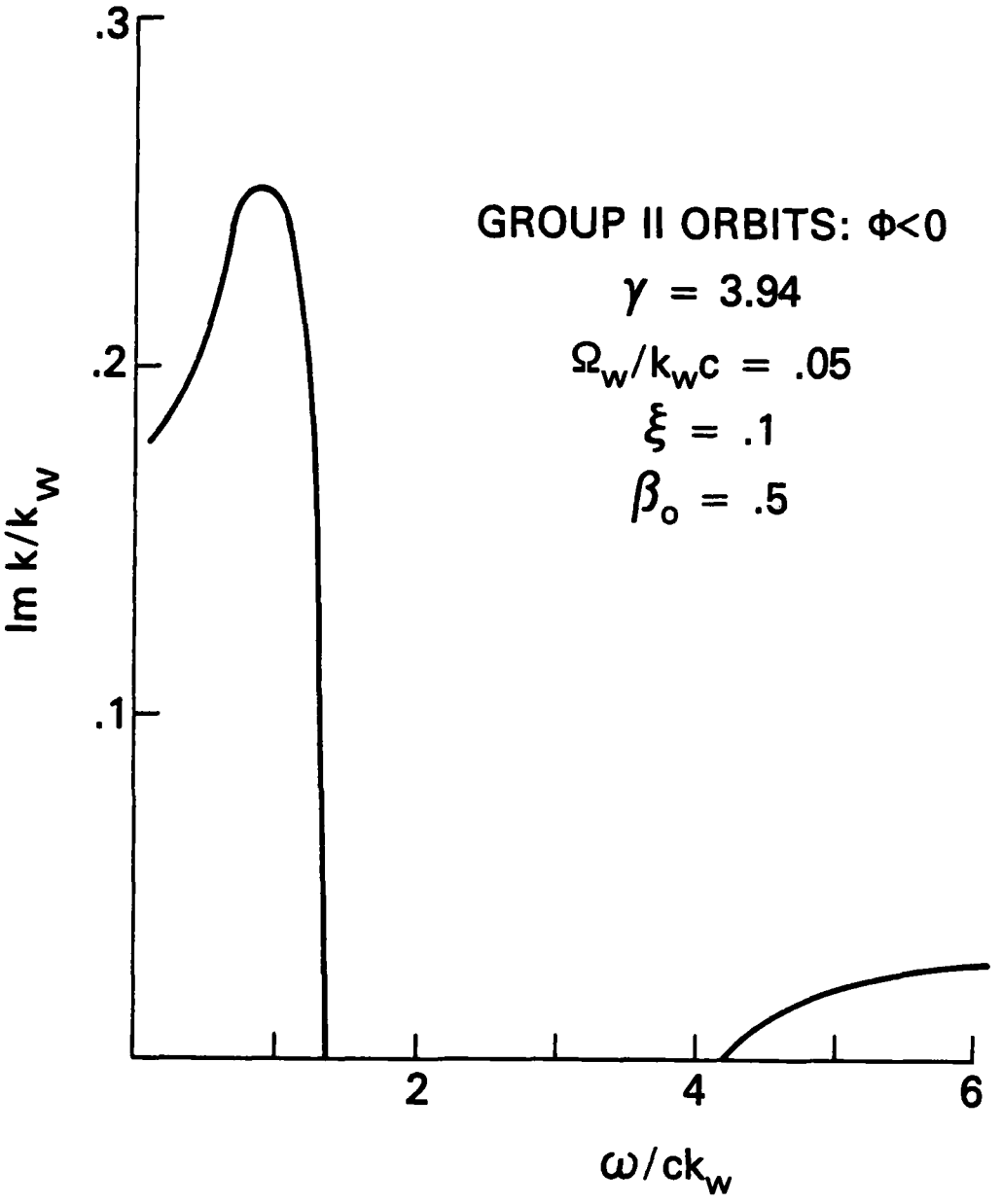

Fig. 9 — Graph of Im k/k_w versus ω/ck_w for group II ($\Phi < 0$) orbits and $\beta_0 = .5$

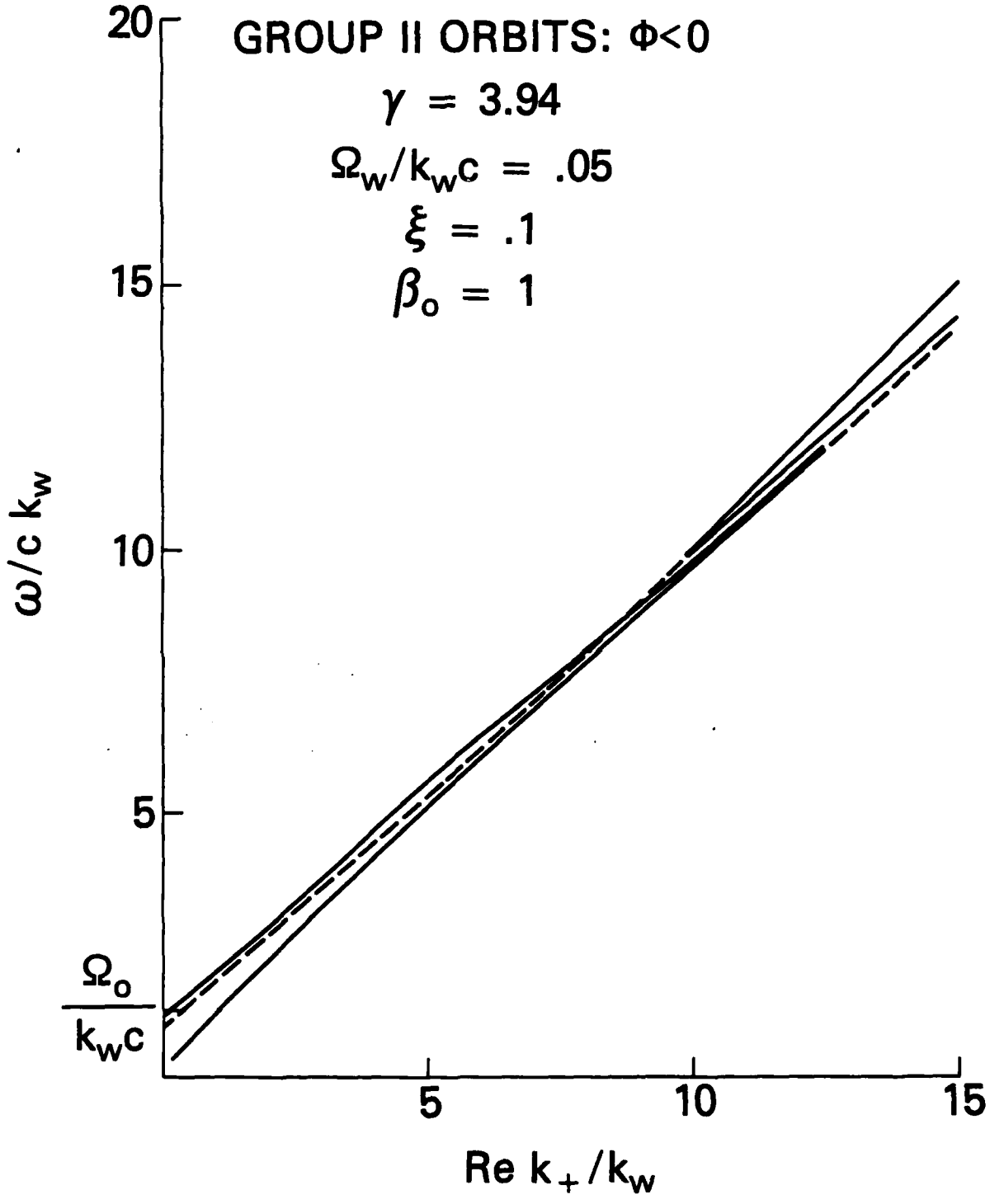

Fig. 10 — Graph of ω/ck_w versus Rek_+/k_w for group II ($\Phi < 0$) orbits and $\beta_0 = 1$

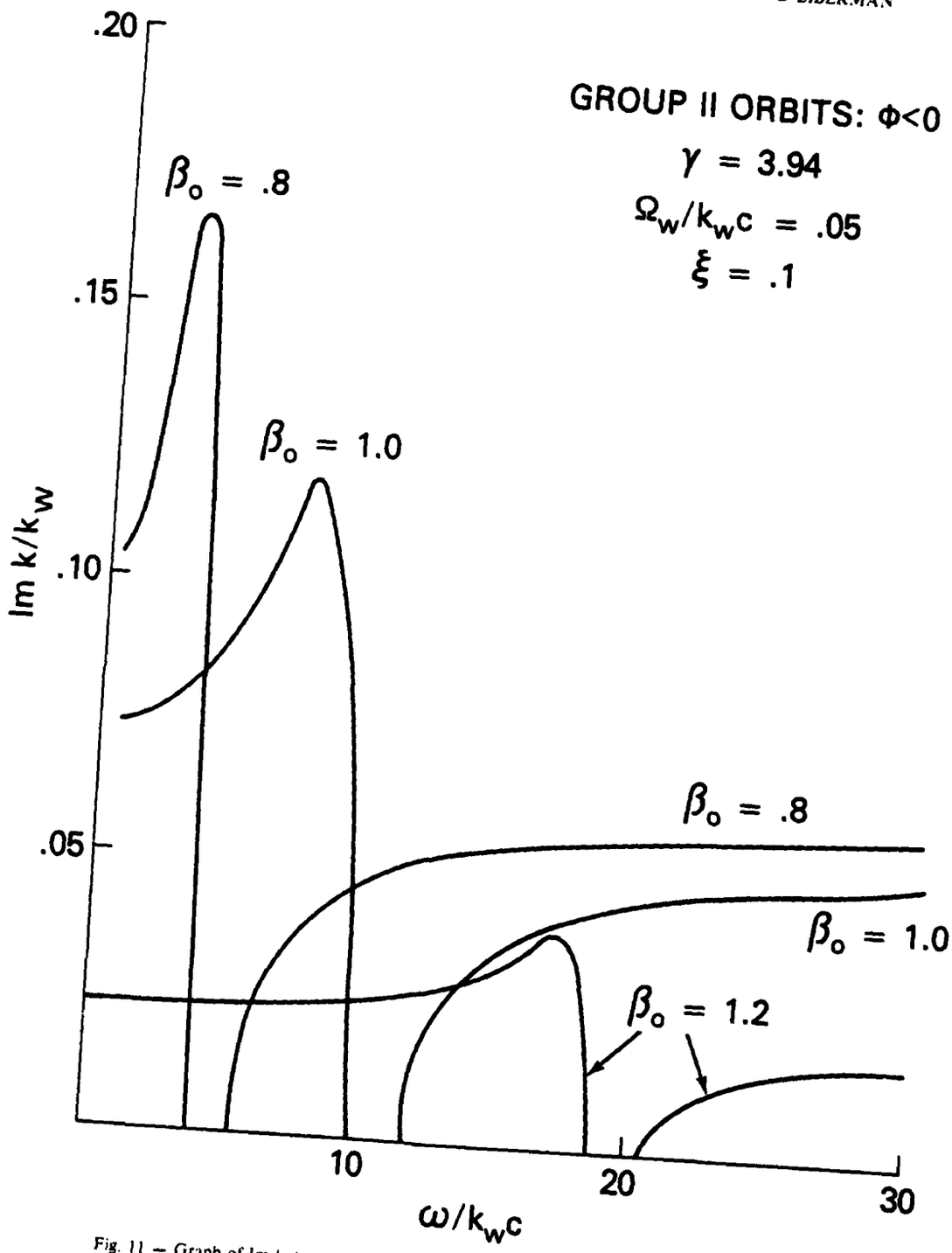

Fig. 11 — Graph of Im k/k_w versus ω/ck_w for group II ($\Phi < 0$) orbits and $\beta_0 = .8$, 1, and 1.2

DISTRIBUTION LIST*

Naval Research Laboratory
4555 Overlook Avenue, S.W.
Washington, D.C. 20375

Attn: Code 1000 - CAPT. E. E. Henifin
1001 - Dr. A. Berman
4700 - Dr. S. Ossakow (26 copies)
4701 - Mr. J. Brown
4740 - Dr. V. L. Granatstein (20 copies)
4740 - Dr. R. K. Parker (20 copies)
4740 - Dr. K. R. Chu
4740 - Dr. C. W. Roberson
4790 - Dr. P. Sprangle (100 copies)
4790 - Dr. C. M. Tang
4790 - Dr. M. Lampe
4790 - Dr. W. M. Manheimer
6603S- Dr. W. W. Zachary
6650 - Dr. L. Cohen
6656 - Dr. N. Seeman
6850 - Dr. L. R. Whicker
6805 - Dr. S. Y. Ahn
6875 - Dr. R. Wagner

On Site Contractors:
Code 4740 - Dr. L. Barnett (B-K Dynamics)
4740 - Dr. D. Dialetis (SAI)
4740 - Dr. Y. Y. Lau (SAI)
4790 - Dr. A. T. Drobot (SAI)
4790 - Dr. J. Vomvoridis (JAYCOR)
4790 - Dr. H. Freund (SAI)

* Every name listed on distribution gets one copy except for those where extra copies are noted.

Dr. Tony Armstrong
SAI, Inc.
P. O. Box 2351
La Jolla, CA 92038

Dr. Robert Behringer
ONR
1030 E. Green
Pasadena, CA 91106

Dr. G. Bekefi (5 copies)
Massachusetts Institute of Technology
Bldg. 26
Cambridge, MA 02139

Dr. Arden Bement (2 copies)
Deputy Under Secretary of Defense
for R&AT
Room 3E114, The Pentagon
Washington, D.C. 20301

Dr. T. Berlincourt
Code 420
Office of Naval Research
Arlington, VA 22217

Dr. I. B. Bernstein (2 copies)
Yale University
Mason Laboratory
400 Temple Street
New Haven, CT 06520

Dr. Charles Brau (2 copies)
Applied Photochemistry Division
Los Alamos National Scientic
Laboratory
P. O. Box 1663, M.S. - 817
Los Alamos, NM 87545

Dr. R. Briggs (L-71)
Lawrence Livermore National Lab.
P. O. Box 808
Livermore, CA 94550

Dr. Fred Burskirk
Physics Department
Naval Postgraduate School
Monterey, CA 93940

Dr. K. J. Button
Massachusetts Institute of Technology
Francis Bitter National Magnet Lab.
Cambridge, MA 02139

Dr. Gregory Canavan
Director, Office of Inertial Fusion
U. S. Department of Energy
M.S. C404
Washington, D.C. 20545

Prof. C. D. Cantrell
Center for Quantum Electronics
& Applications
The University of Texas at Dallas
P. O. Box 688
Richardson, TX 75080

Dr. Maria Caponi
TRW, Building R-1, Room 1070
One Space Park
Redondo Beach, CA 90278

Dr. J. Cary
Los Alamos National Scienific
Laboratory
MS 608
Los Alamos, NM 87545

Dr. Weng Chow
Optical Sciences Center
University of Arizona
Tucson, AZ 85721

Dr. Peter Clark
TRW, Building R-1, Room 1096
One Space Park
Redondo Beach, CA 90278

Dr. Robert Clark
P. O. Box 1925
Washington, D.C. 20013

Dr. William Colson
Quantum Institute
Univ. of California at Santa Barbara
Santa Barbara, CA 93106

Dr. William Condell
Code 421
Office of Naval Research
Arlington, VA 22217

Dr. Richard Cooper
Los Alamos National Scientific
Laboratory
P. O. Box 1663
Los Alamos, NM 87545

Cmdr. Robert Cronin
NFOIO Detachment, Suitland
4301 Suitland Road
Washington, D.C. 20390

Dr. R. Davidson (5 copies)
Plasma Fusion Center
Massachusetts Institute of Technology
Cambridge, MA 02139

Dr. John Dawson (2 copies)
Physics Department
University of California
Los Angeles, CA 90024

Dr. David Deacon
Physics Department
Stanford University
Stanford, CA 94305

Defense Technical Information Center (12 copies)
Cameron Station
5010 Duke Street
Alexandria, VA 22313

Dr. Francesco De Martini
Instituto de Fiscia
G. Marconi" Univ.
Piazzo delle Science, 5
ROMA00185 ITALY

Prof. P. Diament
Columbia University
Dept. of Electrical Engineering
New York, NY 10027

Prof. J. J. Doucet (5 copies)
Ecole Polytechnique
91128 Palaiseau
Paris, France

Dr. John Elgin (2 copies)
Imperial College
Dept. of Physics (Optics)
London SWF, England

Dr. Luis R. Elias (2 copies)
Quantum Institute
University of California
Santa Barbara, CA 93106

Dr. David D. Elliott
SRI International
33 Ravenswood Avenue
Menlo Park, CA 94025

Dr. Jim Elliot (2 copies)
X-Division, M.S. 531
Los Alamos National Scientific Laboratory
Los Alamos, NM 87545

Director (2 copies)
National Security Agency
Fort Meade, MD 20755
ATTN: Mr. Richard Foss, A42

Dr. Robert Fossum, Director
DARPA
1400 Wilson Boulevard
Arlington, VA 22209 (2 copies)

Dr. Edward A. Frieman
Director, Office of Energy Research
U. S. Department of Energy
M.S. 6E084
Washington, D.C. 20585

Dr. George Gamota (3 copies)
OUSDRE (R&AT)
Room 3D1067, The Pentagon
Washington, D.C. 20301

Dr. Richard L. Garwin
IBM, T. J. Watson Research Center
P. O. Box 218
Yorktown Heights, NY 10598

Dr. Edward T. Gerry, President
W. J. Schafer Associates, Inc.
1901 N. Fort Myer Drive
Arlington, VA 22209

Dr. Avraham Gover
Tel Aviv University
Fac. of Engineering
Tel Aviv, ISRAEL

Mr. Donald L. Haas, Director
DARPA/STO
1400 Wilson Boulevard
Arlington, VA 22209

Dr. P. Hammerling
La Jolla Institute
P. O. Box 1434
La Jolla, CA 92038

Director
National Security Agency
Fort Meade, MD 20755
ATTN: Mr. Thomas Handel, A243

Dr. William Happer
560 Riverside Drive
New York City, NY 10027

Dr. Robert J. Hermann
Assistant Secretary of the
Air Force (RD&L)
Room 4E856, The Pentagon
Washington, D.C. 20330

Dr. Rod Hiddleston
KMS Fusion
Ann Arbor, MI 48106

Dr. J. L. Hirshfield (2 copies)
Yale University
Mason Laboratory
400 Temple Street
New Haven, CT 06520

Dr. R. Hofland
Aerospace Corp.
P. O. Box 92957
Los Angeles, CA 90009

Dr. Fred Hopf
University of Arizona
Tucson, AZ 85721

Dr. Benjamin Huberman
Associate Director, OSTP
Room 476, Old Executive Office Bldg.
Washington, D.C. 20506

Dr. S. F. Jacobs
Optical Sciences Center
University of Arizona
Tucson, AZ 85721

Dr. S. Johnston
Dept of Electrical Engineering
Columbia University
N.Y., N.Y. 10027

Mr. Eugene Kopf
Principal Deputy Assistant
Secretary of the Air Force (RD&L)
Room 4E964, The Pentagon
Washington, D.C. 20330

Prof. N. M Kroll
La Jolla Institutes
P. O. Box 1434
La Jolla, CA 92038

Dr. Tom Kuper
Optical Sciences Center
University of Arizona
Tucson, AZ 85721

Dr. Thomas Kwan
Los Alamos National Scientific
Laboratory
MS608
Los Alamos, NM 87545

Dr. Willis Lamb
Optical Sciences Center
University of Arizona
Tucson, AZ 85721

Mr. Mike Lavan
BMDATC-O
ATTN: ATC-O
P. O. Box 1500
Huntsville, AL 35807

Dr. John D. Lawson (2 copies)
Rutherford High Energy Lab.
Chilton
Didcot, Oxon OX11 OOX
ENGLAND

Mr. Ray Leadabrand
SRI International
333 Ravenswood Avenue
Menlo Park, CA 94025

Mr. Barry Leven
NISC/Code 20
4301 Suitland Road
Washington, D.C. 20390

Dr. Donald M. LeVine (3 copies)
SRI International
16[illegible] N. Kent Street
Arlington, VA 22209

Dr. Anthony T. Lin
University of California
Los Angeles, CA 90024

Director (2 copies)
National Security Agency
Fort Meade, MD 20755
ATTN: Mr. Robert Madden, R/SA

Dr. John Madey
Physics Department
Stanford University
Stanford, CA 94305

Dr. Joseph Mangano
DARPA
1400 Wilson Boulevard
Arlington, VA 22209

Dr. S. A. Mani
W. J. Schafer Associates, Inc.
10 Lakeside Office Park
Wakefield, MA 01880

Dr. Mike Mann
Hughes Aircraft Co.
Laser Systems Division
Culver City, CA 90230

Dr. T. C. Marshall
Applied Physics Department
Columbia University
New York, NY 10027

Mr. John Meson
DARPA
1400 Wilson Boulevard
Arlington, VA 22209

Dr. Pierre Meystre
Projektgruppe fur Laserforschung
Max Planck Gesellschaft
Garching, MUNICH WEST GERMANY

Dr. Gerald T. Moore
Optical Sciences Center
University of Arizona
Tucson, Az 85721

Dr. Philip Morton
Stanford Linear Accelerator Center
P. O. Box 4349
Stanford, CA 94305

Dr. Jesper Munch
TRW
One Space Park
Redondo Beach, CA 90278

Dr. George Neil
TRW
One Space Park
Redondo Beach, CA 90278

Dr. Kelvin Neil
Lawrence Livermore National Lab.
Code L-321, P. O. Box 808
Livermore, CA 94550

Dr. Brian Newnam
MS 564
Los Alamos National Scientific
Laboratory
P. O. Box 1663
Los Alamos, NM 87545

Dr. Milton L. Noble (2 copies)
General Electric Company
G. E. Electric Park
Syracuse, NY 13201

Prof. E. Ott (2 copies)
University of Maryland
Dept. of Physics
College Park, MD 20742

Dr. Richard H. Pantell
Stanford University
Stanford, CA 94305

Dr. Claudio Parazzoli
Highes Aircraft Company
Building 6, MS/C-129
Centinela & Teale Streets
Culver City, CA 90230

Dr. Richard M. Patrick
AVCO Everett Research Lab., Inc.
2385 Revere Beach Parkway
Everett, MA 02149

Dr. Claudio Pellegrini
Brookhaven National Laboratory
Associated Universities, Inc.
Upton, L.I., NY 11973

The Honorable William Perry
Under Secretary of Defense (R&E)
Office of the Secretary of Defense
Room 3E1006, The Pentagon
Washington, D.C. 20301

Dr. Alan Pike
DARPA/STO
1400 Wilson Boulevard
Arlington, VA 22209

Dr. Hersch Pilloff
Code 421
Office of Naval Research
Arlington, VA 22217

Dr. Charles Planner
Rutherford High Energy Lab.
Chilton
Didcot, Oxon, OX11, 00X
ENGLAND

Dr. Michal Poole
Daresbury Nuclear Physics Lab.
Daresbury, Warrington
Cheshire WA4 4AD
ENGLAND

Dr. Don Prosnitz
Lawrence Livermore National Lab.
Livermore, CA 94550

Dr. D. A. Reilly
AVCO Everett Research Lab.
Everett, MA 02149

Dr. James P. Reilly
W. J. Schafer Associates, Inc.
10 Lakeside Office Park
Wakefield, MA 01880

Dr. A. Renieri
C.N.E.N.
Div. Nuove Attivita
Dentro di Frascatti
Frascatti, Rome
ITALY

Dr. Daniel N. Rogovin
SAI
P. O. Box 2351
La Jolla, CA 92038

Dr. Michael Rosenblum
MIT - Magnet Laboratory
Cambridge, MA 02139

Dr. Marshall N. Rosenbluth
Institute for Advanced Study
Princeton, NJ 08540

Dr. Eugene Ruane (2 copies)
P. O. Box 1925
Washington, D.C. 20013

Dr. Antonio Sanchez
MIT/Lincoln Laboratory
Room B231
P. O. Box 73
Lexington, MA 02173

Dr. Aleksandr N. Sandalov
Department of Physics
Moscow University
MGU, Lenin Hills
Moscow, 117234, USSR

Prof. S. P. Schlesinger
Columbia University
Dept. of Electrical Engineering
New York, NY 10027

Dr. Howard Schlossberg
AFOSR
Bolling AFB
Washington, D.C. 20332

Dr. Stanley Schneider
Rotodyne Corporation
26628 Fond Du Lac Road
Palos Verdes Peninsula, CA 90274

Dr. Marlan O. Scully
Optical Science Center
University of Arizona
Tucson, AZ 85721

Dr. Steven Segel
KMS Fusion
3621 S. State Street
P. O. Box 1567
Ann Arbor, MI 48106

Dr. Robert Sepucha
DARPA/STO
1400 Wilson Boulevard
Arlington, VA 22209

Dr. A. M. Sessler
Lawrence Berkeley Laboratory
University of California
1 Cyclotron Road
Berkeley, CA 94720

Dr. Earl D. Shaw
Bell Labs
600 Mountain Avenue
Murray Hill, NJ 07974

Dr. R. Shefer
Massachussetts Institute of
Technology
Bldg. 26
Cambridge, MA 02139

Dr. Chan-Chin Shih
R&D Associates
P. O. Box 9695
Marina Del Rey, CA 92091

Dr. Jack Slater
Mathematical Sciences, NW
P. O. Box 1887
Bellevue, WA 98009

Dr. Kenneth Smith
Physical Dynamics, Inc.
P. O. Box 556
La Jolla, CA 92038

Mr. Todd Smith
Hansen Labs
Stanford University
Stanford, CA 94305

Dr. Joel A. Snow
Senior Technical Advisor
Office of Energy Research
U. S. Department of Energy, M.S. E084
Washington, D.C. 20585

Dr. Richard Spitzer
Stanford Linear Accelerator Center
P. O. Box 4347
Stanford, CA 94305

Mrs. Alma Spring
DARPA/Administration
1400 Wilson Boulevard
Arlington, VA 22209

DRI/MP Reports Area G037 (2 copies)
333 Ravenswood Avenue
Menlo Park, CA 94025
ATTN: D. Leitner

Dr. Abraham Szoke
Lawrence Livermore National Lab.
MS/L-470, P. O. Box 808
Livermore, CA 94550

Dr. Milan Tekula
AVCO Everett Research Lab.
2385 Revere Beach Parkway
Everett, MA 02149

Dr. John E. Walsh
Department of Physics
Dartmouth College
Hanover, NH 03755

Dr. Wasneski (2 copies)
Naval Air Systems Command
Department of the Navy
Washington, D.C. 20350

Ms. Bettie Wilcox
Lawrence Livermore National Lab.
ATTN: Tech. Info. Dept. L-3
P. O. Box 808
Livermore, CA 94550

Dr. A. Yariv
California Institute of Tech.
Pasadena, CA 91125


ILMED
8